Table of Contents

1. Introduction

In the last decade inorganic-organic hybrid materials have attracted much attention due to their improved properties arising from the synergetic junction of the two components. For instance optimizing mechanical, thermal or optical properties as well as hydrophobicity, permeability, catalytic properties and many more can provide new materials with user-defined features[1-3]. Aim of this work was to find a simple and effective pathway for a covalent connection between the inorganic and organic component in such materials. While several methods were used for the covalent connection of the components previously, such as hydrosilation reaction[4-7], copolymerization of functional macromonomers[8,9] or the use of macroinitiators[10,11], this work will study the click chemistry bond formation between inorganic building blocks based on spherosilicates and silsesquioxanes or on mixtures of spherosilicates and polymers. For this purpose full eight corner azide and alkyne modified silica cages were prepared. Azide end-modified poly(methyl methacrylate) and polydimethylsiloxane with alkyne end-groups were used as polymeric matrices. The two components were covalently connected by Huisgen 1,3-dipolar cycloaddition reaction to give a hybrid material.

1.1. Hybrid Materials

Although polymers offer a lot of advantages such as good processability, toughness and low cost, their field of application is limited because they are rather soft and many times their thermal and chemical stability is limited. The homogenous incorporation of inorganic components into polymers on the nanometer scale creates materials with new properties favourably combining the advantages of the two components. Figure 1.1 shows the properties of different classes of materials and gives an idea of how to combine these materials to obtain new ones with improved properties.

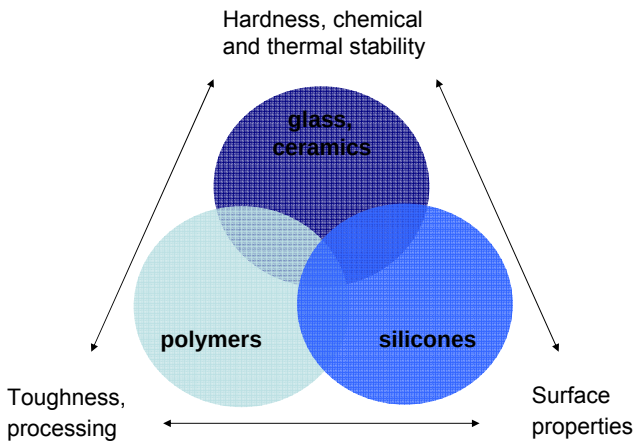

For example the combination of the properties of ceramics and organic polymers makes it possible to obtain materials with good processability and toughness that are nevertheless hard and thermally and chemically stable.

Figure 1.1: Properties of materials

Mechanical and thermal stability are only a part of various properties that can be improved by combining two different materials on the nanometer scale. Choosing the right components it is also possible to define surface properties, pore sizes[12], permeability[13], electric[14] and magnetic[15] properties, flammability[16] and many more[2].

1.1.1. Applications for Hybrid Materials

Inorganic-organic hybrid materials can combine the often dissimilar features of the different components in one material. The diversity of both classes of components provides the possibility to design materials with the requested properties and results in a very broad field of applications[2].

In nature hybrid materials are widespread: e.g. bones and sea shells consist of inorganic components embedded in an organic matrix[17]. The oldest man-made hybrid material is Maya blue, which is a class I hybrid material consisting of clay and indigo dye the Maya used for their paintings. Thanks to this robust hybrid pigment the Maya paintings are characterized by bright blue colours and are nowadays looking almost as fresh as in the 8th century[18].

Nowadays applications are numerous in optics[19], electronics[14,20,21], magnetics[15], membranes[13,22], catalytic[23], dental and medical[24] sector as well as for functional coatings such as antistatic and scratch resistant coatings[25], corrosion protection[2] and solar cells[26].

1.1.2. Classification of Hybrid Materials

Fundamental for the quality of hybrid materials is the homogeneous distribution of both components in the material. In physical mixtures the incompatibility of the two components often causes microphase separation and agglomeration of one component in the matrix of the other. This can be avoided either by functionalization of the surface of the inorganic particles with organic groups[27] or by covalent connection of the two components. Thus, hybrid materials are divided into two classes: Class I hybrid polymers consist of two components that are intimately mixed but do only exhibit weak interaction with each other, such as van-der-Waals contacts, hydrogen bonding, or weak electrostatic interactions. As mentioned above, these materials can show microphase separation. Class II hybrid materials avoid this demixing phenomenon by strong chemical interaction between the two components. Figure 1.2 shows the difference between Class I and Class II hybrid materials.

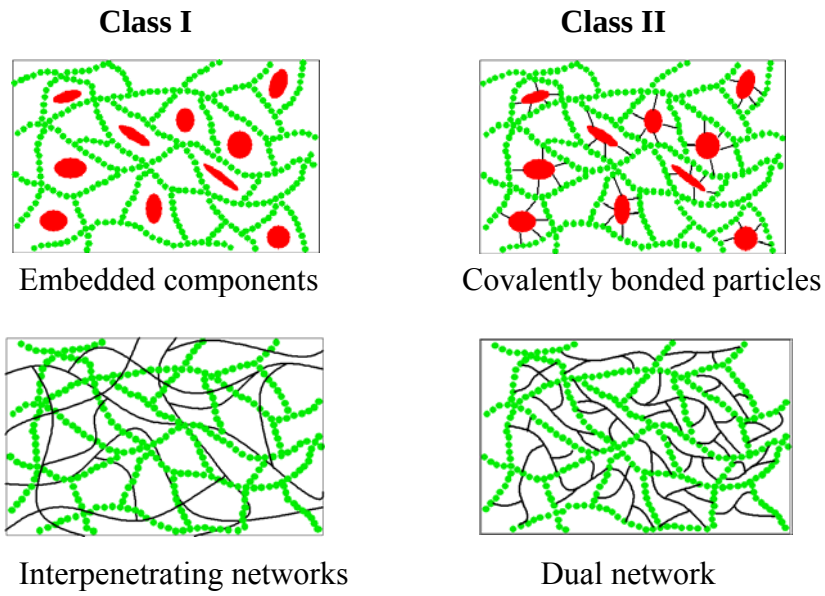

Figure 1.2: Different classes of hybrid materials

Class I hybrid polymers can be obtained either by intimate mixing of the preformed components e.g. by extrusion, or by mixing of the precursors and simultaneous preparation of the inorganic and organic phase. One of the most versatile methods for the preparation of the inorganic component is the sol-gel process, which is a method to obtain an inorganic oxide based material by hydrolysis and condensation of molecular precursors[28](see part 1.2.1). Sol-gel precursors can be modified with organic groups in

order to improve the compatibility with the organic polymer and thus to reduce microphase separation[27]. The modification of the sol-gel precursor with polymerizable groups[8,9,29] is the most common method for the preparation of class II hybrid polymers, but also hydrosilation reaction[5-7] and many other reactions[30,31] are used to create a covalent bond between the inorganic and the organic component.

1.1.3. Nanocomposites

Nanocomposites are materials containing both inorganic and organic components, where one of the structural units is in a size range of 1-100 nm, while the units in hybrid materials are rather molecular building blocks. Thus, there is no concrete borderline to distinguish between nanocomposites and hybrid materials, because a large molecular building block of a hybrid material can already be in the nanometer size range.

Size matters: There are two major effects related to the size of objects[32] that can change dramatically when the object approaches the nanometer length scale. If the size is in the nanometer regime, electronic changes occur leading to the so called quantum size effects. Furthermore, the surface to volume ratio increases dramatically, leading to an increasing importance of the surface atoms regarding the overall properties of the materials.

1.2. Silica Nanobuilding Blocks

Among the most important inorganic nanobuilding blocks are silica nanoparticles, due to the high stability of Si-O-Si and Si-C bonds as well as the high reactivity of Si-halogen and Si-alkoxide bonds, which can be used for the introduction of organic groups. Defined silica compounds are even more versatile than the nanoparticles, because these compounds have the additional advantages of easy accessibility and a well defined structure in the nanometer size regime. Typical structures are cages that can be described by the formula $[RSiO_{1.5}]_n$ (silsesquioxanes) or $[SiO_2]_n$ (spherosilicates), where n can be 6-18. The most important of these cubes are the octamers $[RSiO_{1.5}]_8$ (polyhedral oligomeric silsesquioxanes, POSS) and $[SiO_2]_8$ (spherosilicate) with a diameter of about 1 nm.

Polyhedral Oligosilsesquioxane (POSS) **Spherosilicate**

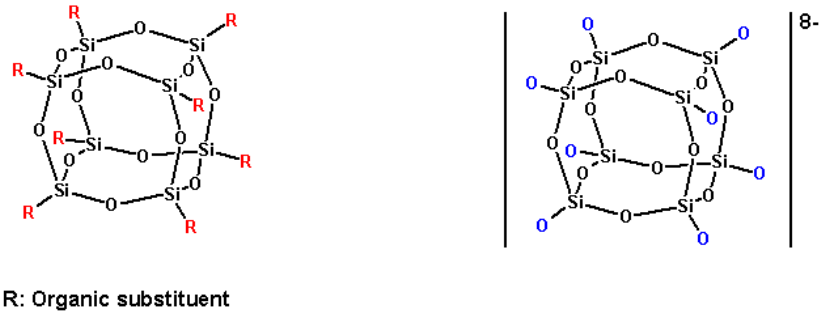

Figure 1.3: Silica nanobuilding blocks

Cubic silsesquioxanes and functionalized spherosilicates are the smallest silica particles possible having a well-defined silica core surrounded by eight organic groups. Due to their small and defined sizes as well as the high density of functional groups and their rigid framework, silica cages are very prominent in materials chemistry[9,16,33-40]. Especially the eight corner functionalization with polymers is a versatile tool to well defined star-polymers, which offer lower melt and solution viscosities compared to linear polymers[41].

1.2.1. Preparation of Silica Cages: Sol-Gel Process

The sol-gel process is a method for the preparation of ceramic materials under mild reaction conditions, which also allows the incorporation of organic functional groups, because the Si-C bond is hydrolytically stable. Precursors for the sol-gel process are inorganic salts or (semi)metal alkoxides. Hydrolysis and condensation reactions lead to the formation of a sol, which is a colloidal phase that consists of oxide particles of a few nanometers in size. Further hydrolysis and condensation reactions leads to the formation of a so-called gel, a continuous network enclosing a liquid phase.

The sol-gel process for silicon alkoxides was studied extensively and requires four components: a silicon alkoxide, water, an acidic or basic catalyst, and a solvent to provide compatibility between the usually immiscible silicon alkoxide and water.

The sol-gel process for metal alkoxides is generally related to that of the silicon based system, but will not be discussed in this work.

The sol-gel process starts with the hydrolysis of a silicon alkoxide which forms a silanol species. These compounds are not stable and condense. Under stoichiometric ratio, the alcohol producing condensation reaction is favoured, while for larger hydrolysis ratio a water releasing condensation is dominant.

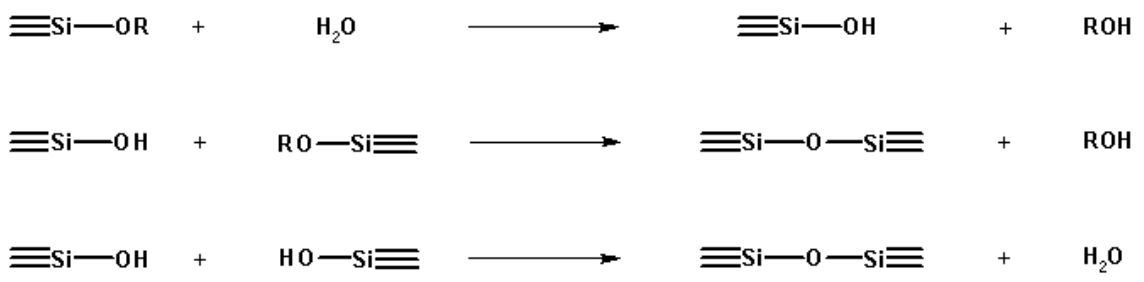

Scheme 1.1: Hydrolysis and Condensation of Si-alkoxides

Acid or base catalysts are widely used in sol-gel chemistry of silicon alkoxides to accelerate the hydrolysis reactions and to obtain shorter gelation times.

Due to its mild reaction conditions and inertness towards many organic functionalities, the sol-gel process is one of the most important pathways for the preparation of oxide compounds, especially for silica nanoparticles. Similar reaction steps, i.e. hydrolysis and condensation of silicon alkoxides are taking place in the synthesis of the cage compounds, however, no sol-gel transition is observed for these compounds.

1.2.1.1. Synthesis of Spherosilicates

Special methods have been developed which allow the selective synthesis of silica cages by controlled hydrolysis and condensation. Spherosilicates were obtained in low yields using tetraalkoxysilanes as precursors until *Hoebbel et al.*[42] found a simple and efficient method for the synthesis of the tetramethylammonium silicate, octaanion $[Si_8O_{12}^{8-}]((CH_3)_4N^+)_8$. It is nowadays well known that in aqueous solutions containing tetraalkylammonium ions, random polymerization of silicate anions is suppressed and the anions with specific cage-like structures are formed selectively, depending on the type of alkyl group[43]. Tetramethylammonium ion as well as (2-hydroxyethyl)trimethylammonium

ion contribute to the formation of the cubic octamer $[Si_8O_{12}^{8-}]((CH_3)_4N^+)_8$. The thus obtained octaanion can be modified with organic groups by reaction with chlorosilanes, the most important ones being chlorodimethylsilane or chlorodimethylvinylsilane, both of whom provide groups that can be further functionalized by hydrosilation reaction as it is shown in Figure 1.4. Up to now various other different functional and non-functional groups have been attached[44], such as trimethylsilane[42], phenyldimethylsilane[45], (chloromethyl)dimethylsilane[45], bromodimethylsilane[46], including also two different moieties on one cage. However, the latter materials consist typically of a statistical average of the applied groups[47]. Furthermore, the dimethylsilyl group can be substituted by other silyl groups[48].

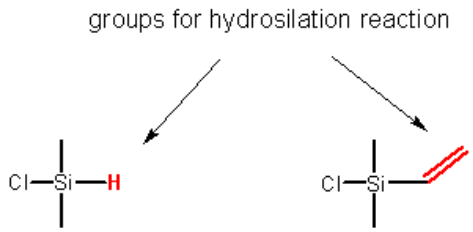

Chlorodimethylsilane reacts with the anion of the cage and provides a Si-H bonding for the hydrosilation of allyl-compounds. Chlorodimethylvinylsilane provides a double bond, which can undergo hydrosilation reaction.

Figure 1.4: Chlorosilanes

Hydrosilation reaction of the two cages with each other results in highly porous materials[40].

1.2.1.2. Synthesis of Polyhedral Oligomeric Silsesquioxanes (POSS)

The first one to discover the existence of compounds with the formula $[RSiO_{1.5}]_n$ was *Ladenburg* in 1873[49]. Nevertheless only in 1946 *Scott et al.*[50] were able to find a controlled synthesis and in 1955 *Barry and co-workers* described the structures of these compounds[51]. Since then the main synthetic route was the hydrolysis and condensation reactions of organotrichlorosilanes under basic or acidic conditions. In order to obtain shorter reaction times and higher yields the synthesis has been improved using e.g. benzyltrimethylammonium hydroxide[52] or tetrabutylammonium fluoride (TBAF)[53] as bases.

Incompletely condensed silsesquioxanes can be obtained by hydrolytic condensation of cyclohexyltrichlorosilane in aqueous acetone as it is shown in Scheme 1.2. The silanol compound **a** can be obtained in 60-70% yield and can be separated from the by-products taking advantage of their different solubility[54].

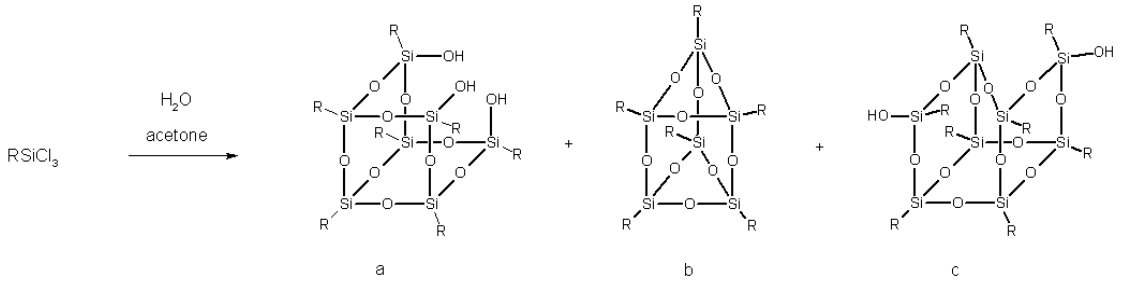

Scheme 1.2: Preparation of incompletely condensed silsesquioxanes

Reacting compound **a** with functional organotrichlorosilanes provides the possibility to obtain POSS with only one functional (e.g. polymerizable see Scheme 1.4) group. Applying this pathway various one corner functional POSS cages have been prepared[38].

1.2.1.3. Hydrosilation Reaction

The most versatile reaction for silicon-carbon bond formation is the hydrosilation reaction, a platinum-catalyzed addition reaction between a terminal double bond and a hydrosilane, first discovered by *Speier* in 1957[55].

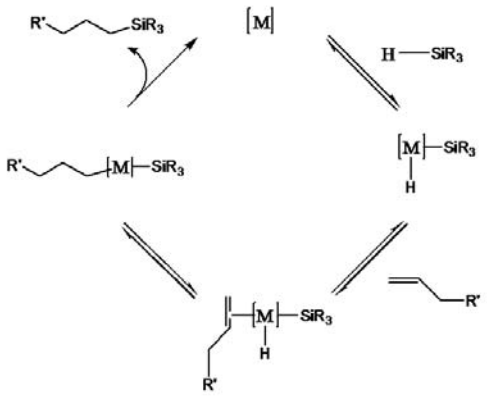

The mechanism as it is shown in Scheme 1.3 was proposed by *Chalk and Harrod* in 1965[56] and describes a catalytic cycle based on oxidative addition of silane and subsequent alkene coordination to the metal centre. The next step is a migratory insertion between a metal-element bond followed by reductive elimination.

Scheme 1.3: Chalk-Harrod Mechanism for Hydrosilation reactions

A variety of platinum compounds have been used as catalysts for the hydrosilation reaction, the most versatile ones being Speier's hexachloroplatinic acid and Karstedt's catalyst, platinum-1,3-divinyl-1,1,3,3-tetramethyldisiloxane complex[57].

1.2.2. Nanocomposites containing Silica Cages

POSS cages or spherosilicates incorporated in an organic (polymeric) matrix can be referred to as nanocomposites and hybrid materials because they are exactly at the borderline, as the silica cages are molecular building blocks in the nanometer size range.

Nanocomposites based on silica cages have recently gained considerable interest because the cages can be modified with a wide variety of functional groups. Especially POSS cages are often used due to the easy accessibility of cages with differently substituted corners (see Scheme 1.4), which allows the formation of materials with various different morphologies[7,38,58].

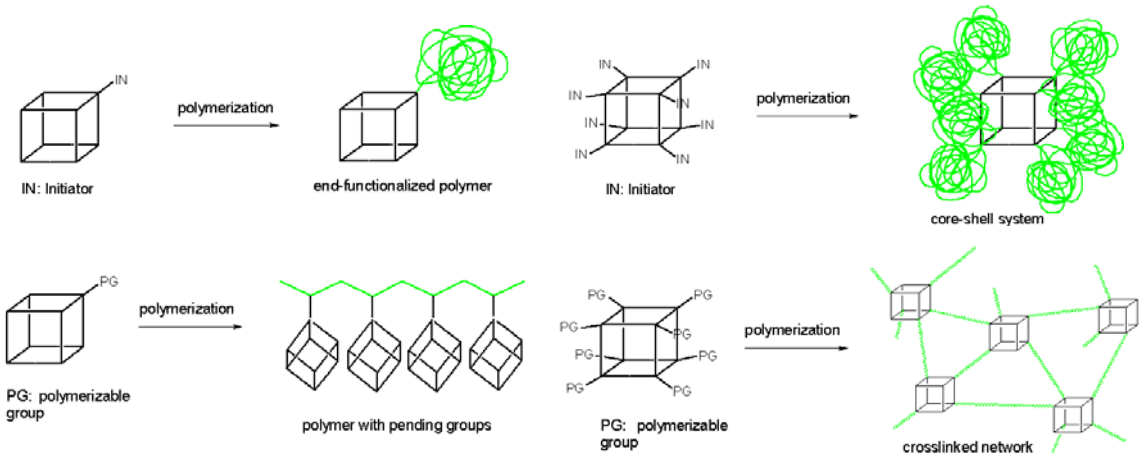

Scheme 1.4: Nanocomposites with POSS cages

While one or two functional groups result in linear macromolecules, cages having more than two functional groups can build crosslinked polymers with properties differing from the former. For example, POSS cages with one polymerizable group can be used as monomers and by (co-)polymerization linear macromolecules with pending inorganic groups can be prepared[8,29,59,60]. If more than two corners of the cage are bearing a polymerizable group, the cage can act as a crosslinker[33,37]. Moreover the cages can be furnished with an initiating group on one or more corners in order to obtain end-functionalized polymers and core-shell systems or star polymers respectively[61,62] (see Scheme 1.4).

Up to now POSS cages have been incorporated into a variety of polymers, such as polyacrylics[9], polyolefins[8], polystyrene[60], polyurethanes[63] and many more. The obtained

hybrid polymers often show improved mechanical and chemical stability as well as changes in vicosity[59] and electronic properties. Moreover, characteristic architectural features, such as core-shell systems, often result in improved processing properties. Thus, these nanocomposites are attractive for applications in high performance hybrid materials, such as liquid crystals[64], CVD-coatings[65], photoresists[66] and many more.

1.3. Atom Transfer Radical Polymerization (ATRP)

One of the most versatile polymerization techniques in the preparation of hybrid materials is the free radical polymerization, because of its robustness and broad usability. Free radical polymerization is an uncontrolled polymerization technique. Due to the high reactivity of the radical it does not only add monomers but it can also combine with another radical or disproportionate. The polymers obtained usually have high molecular weight distributions and the molecular weight cannot be predicted. For this reason several techniques have been developed allowing the radical polymerization to be controlled. Living radical polymerization techniques are based on an equilibrium between the radical and a dormant species[67]. Thus the concentration of radicals is considerably reduced and thus the possibility that two radicals react with each other can be reduced. ATRP uses halogen-atom containing compounds as dormant species, which can be activated by abstraction of the halogen by a catalyst[68] (Scheme 1.5). The equilibrium can be shifted by the catalyst system used.

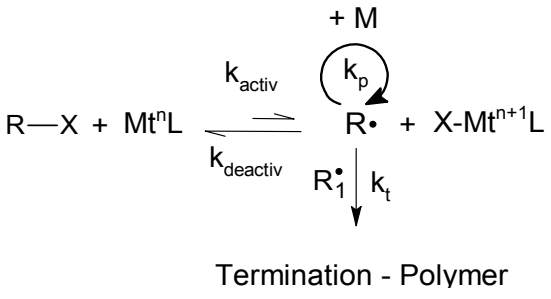

For a living polymerization it is important to shift the equilibrium to an overbalance of the dormant species and thus the concentration of radicals is reduced.

Scheme 1.5: Mechanism of ATRP

Besides reducing the molecular weight distributions, the controlled polymerization techniques offer the possibility to prepare polymers and copolymers with defined structures, such as block copolymers, star and graft systems and dendrimers[69]. These

structures have a considerable effect on the properties of the polymers and thus open new fields of application.

Additionally ATRP allows to obtain polymers with halogen end-groups which can easily be modified by substitution reactions. Polymers with various functional end-groups, such as hydroxyl[70], allyl[71], hydrogen[72], oxazoline[73], maleic anhydride[71], azides[74], amines[75] and nitriles have already been prepared by ATRP and a subsequent substitution reaction.

1.4. Click Chemistry

In nature, carbon-heteroatom links are preferred over carbon-carbon links, because nature's starting material is carbon dioxide and its reaction solvent is water. *Sharpless* and co-workers[76] were fascinated by the simplicity of the reactions in nature and defined the term 'click chemistry' for a set of powerful and selective reactions that follow nature's lead and provide an effective pathway to new compounds. This new form of chemistry is based on the building block system and joins small (unsaturated) units together by heteroatom links. Since *Sharpless* and co-workers defined the term 'click chemistry' in 2001[76], it has gained considerable interest in all divisions of chemistry[77-80] due to the simplicity and efficiency of these reactions. A click reaction has to fulfil a series of stringent criteria defined by *Sharpless* and his co-workers: 'The reaction must be modular, wide in scope, give very high yields, generate only inoffensive by-products and be stereospecific. The required process characteristics include simple reaction conditions, readily available starting materials, the use of no solvent or a solvent that is benign or easily removed and simple product isolation'[76].

Typical click reactions are

- Cycloadditions of unsaturated species
- Nucleophilic substitution reactions, in particular ring-opening reactions
- 'non-aldol' carbonyl chemistry
- additions to carbon-carbon multiple bonds, such as epoxidation and aziridination

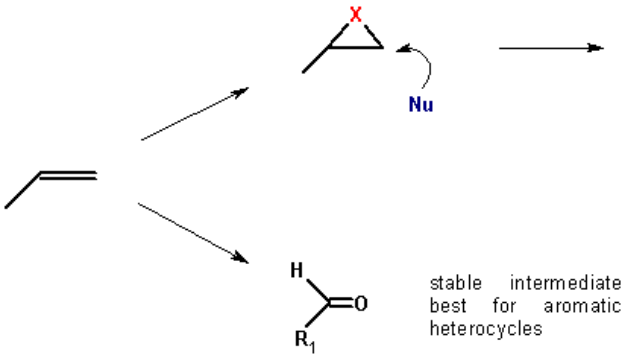

Formation of strained ring systems followed by ring-opening reaction and hydroformylation are typical click reactions[76] (see Scheme 1.6).

Scheme 1.6: Examples for Click Reactions

Cycloaddition reactions involving heteroatoms, such as Hetero-Diels-Alder reactions and 1,3-dipolar cycloadditions have drawn exceptionally much attention to themselves, as they provide a fast access to a variety of five- and six-membered heterocycles. The most versatile of these reactions is the Huisgen 1,3-dipolar cycloaddition reaction[81], which can link various functional groups together, the most important 1,3-dipoles are shown in Figure 1.5. In the last years especially azides and their 1,3-dipolar cycloaddition reactions with alkynes and nitriles have proven to be very promising.

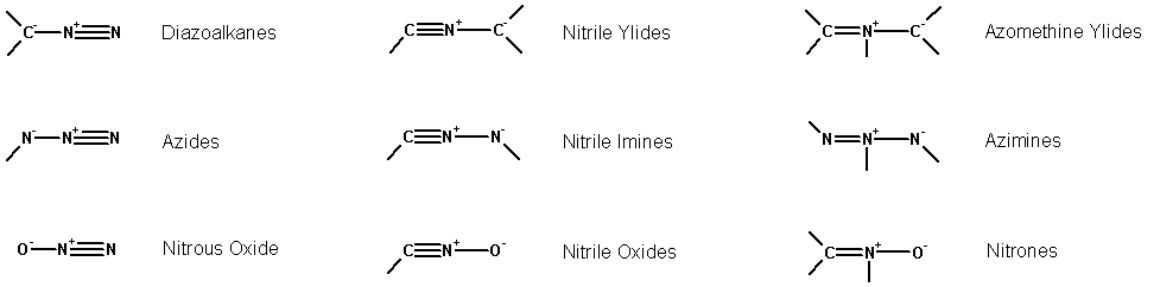

Figure 1.5: 1,3-Dipolar Compounds

The thermal version of this cycloaddition reaction has been studied extensively by *Huisgen* and *Firestone*. Huisgen proposed a concerted mechanism[81-83], in which the 4π electron system of the 1,3-dipol interacts with the π-bond of the dipolarophil (Scheme 1.7a), while Firestone insisted on a stepwise mechanism[84,85] with singlet diradical intermediates (Scheme 1.7b).

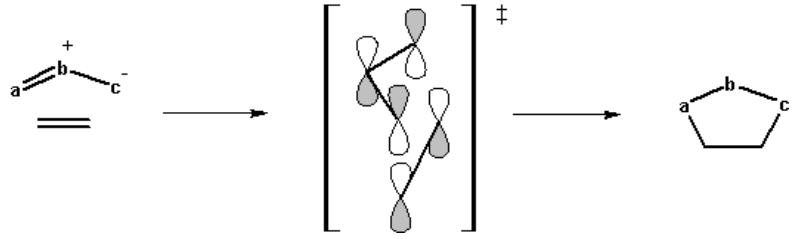

Scheme 1.7a: Concerted mechanism proposed by Huisgen

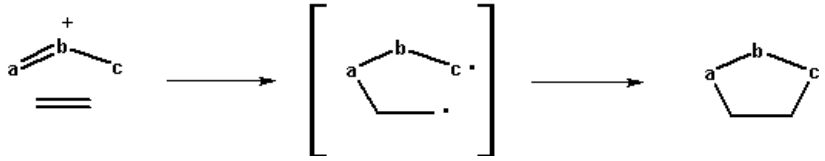

Scheme 1.7b: Stepwise mechanism proposed by Firestone

In 1987, *McDouall*[86] proved by MCSCF (multiconfiguration self-consistent field) studies that the concerted mechanism is preferred, because it exhibits a significantly lower activation barrier than the stepwise mechanism.

The thermal 1,3-dipolar cycloaddition reactions of azides with alkynes are not regioselective and form 1,5- and 1,4-disubstituted triazoles. Thus, *Rostovtsev et al.*[87] in 2002 developed a copper catalyzed version of this reaction that yielded selectively 1, 4-substituted triazoles. Compared to the thermal version of the Huisgen 1,3-dipolar cycloaddition the copper catalyzed process is accelerated 10^7 times by the catalyst and reaches excellent scope and selectivity. There have been many discussions about the mechanism of this reaction[87-94]. It definitely differs from the thermal Huisgen reaction, which is a [2+3] cycloaddition reaction. The density functional theory calculations by *Ahlquvist*[92] point to a binuclear mechanism (see Scheme 1.8). It is based on the initial formation of copper acetylide, followed by attack of the azide on a second copper centre replacing a ligand and only then the azide forms a chemical bond with the acetylide building a seven membered ring. In the last step the catalyst is eliminated from the ring releasing the triazole.

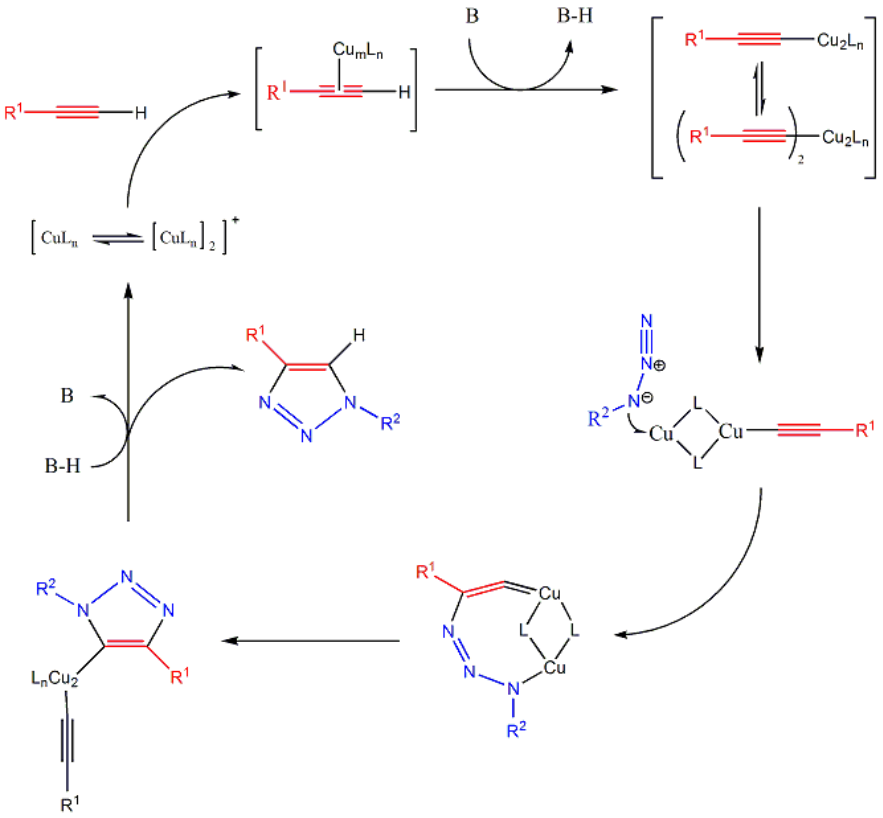

Scheme 1.8: Mechanism of the Huisgen 1,3-dipolar cycloaddition

The rate-determining step is believed to be the formation of the copper metallacycle from a reactive intermediate involving copper-coordinated alkyne and azide. However, the exact nature of the reactive intermediate is unclear[92].

Possible reactive intermediates are (Figure 1.6)[95]:

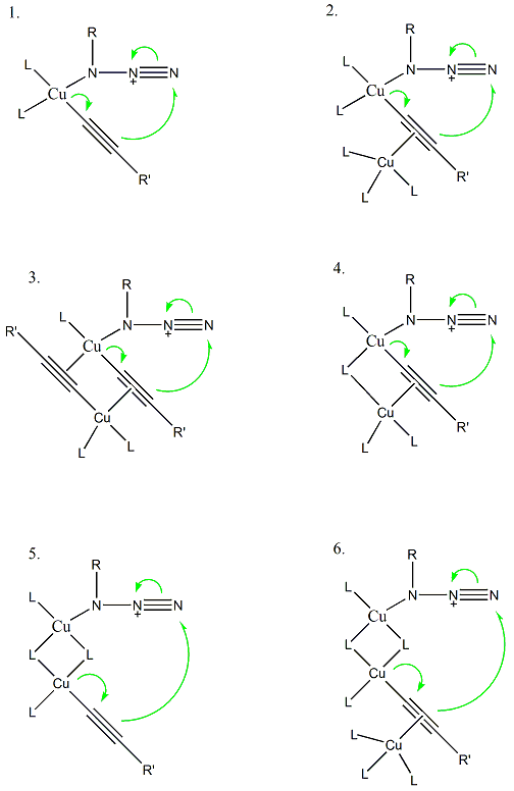

1. Activation by one copper atom
2. Activation by one copper atom and additional π-activation of copper acetylide by a second copper atom
3. Bis-alkyne bridged intermediate
4. Two μ-coordinated copper featuring a π-activated copper acetylide.
5. Azide and alkyne react on two different copper atoms
6. Like 5, with additional π-activated copper acetylide.

Figure 1.6: Possibilities for the Transition State

The first catalyst for the 1,3-dipolar cycloaddition reactions was a copper(I) species formed in situ from copper(II)sulphate and sodium ascorbate. However, since *Chan et al.*[93] discovered an accelerating effect of amine ligands in 2004 a variety of new catalyst systems including activating ligands have been developed[89,96]. Copper species used were for example Cu(II)SO_4/sodium ascorbate, Cu(I)Br, Cu(I)$(MeCN)_4PF_6$, copper metal/NEt_3, copper cluster and many more. Typical ligands that were used for the activation of the copper species are triethylamine, N,N,N',N'',N''-pentamethyldiethylenetriamine (PMDETA) and triazole containing ligands like tris(benzyltriazolylmethyl)amine (TBTA).

1.4.1. Click Reactions in Materials Chemistry

Click reactions have gained considerable interest in many fields of research, such as medicinal chemistry[77], biochemistry[97] and many more[98]. Especially in materials chemistry the Huisgen 1,3-dipolar cycloaddition reaction proved to be a versatile tool for the covalent connection of different polymers or inorganic components and polymers[34,79,80,95,99-105]. Structurally well-defined copolymers as well as hybrid polymers can be obtained with mild reaction conditions and without forming any undesired by-products. Moreover, the building block system provides an easy access to a great variety of new materials as well as a more efficient pathway to well-known substances.

1.5. Organic Azides

Most organic azides are explosive substances that decompose with the release of nitrogen through the slightest input of energy. To be non-explosive the rule for organic azides is that the number of nitrogen atoms must not exceed that of carbon[106]. The structure of azides was suggested to be a 1*H*-triaziridine by *Curtius*[107] and *Hantzsch*[108], but was rapidly revised in favour of linear polar mesomeric structures.

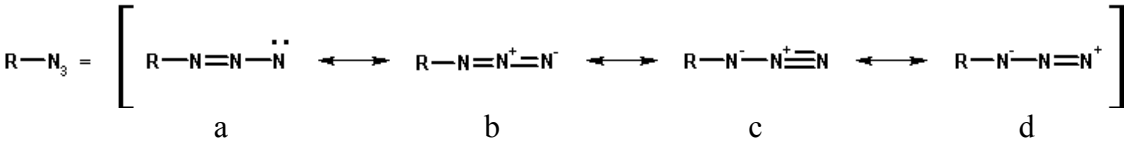

Scheme 1.9: Mesomeric structures of organic azides

The mesomeric structures of the organic azides[106] shown in Scheme 1.9 explain the unique properties of these compounds. The dipolar structures **c** and **d** explain the facile decomposition of azides into nitrene and dinitrogen and also the 1,3-dipolar behaviour of these compounds; Structure **d** also explains the regioselectivity of the reactions with electrophiles and nucleophiles.

Despite their explosive nature organic azides are valuable intermediates in organic synthesis, being used for the synthesis of anilines, as precursors for nitrenes and in the last years through the raise of ‘click reactions’ increasingly for 1,3-dipolar cycloadditions such

as the Huisgen 1,3-dipolar cycloaddition reaction of azides with alkynes as it is shown in Scheme 8.

In this work, the copper catalyzed version of the Huisgen 1,3-dipolar cycloaddition of azides with alkynes (described in part 1.4) was used for the functionalization of defined silica cages (described in part 1.2). The main aim of this work was the introduction of spherosilicates and polyhedral oligomeric silsesquioxanes into organic polymers by click reaction.

2. Aim of this work

Aim of this thesis was the click chemistry bond formation between defined silica cages and organic and inorganic polymers in order to obtain class II inorganic-organic nanocomposites with defined structures by a simple and effective reaction.

The motivation of this approach was the possibility to obtain nanocomposites by a simple reaction that can be carried out using simple reaction conditions and does not give any unwanted by-products. Moreover the building block system provides the possibility of combining the modified spherosilicates arbitrarily with any azide or alkyne functionalized compound.

Major targets of this work were:

- Preparation of eight corner alkyne and azide modified defined silica compounds via a preferably fast, efficient and cheap synthesis pathway.
- A Model click reaction with an eight corner alkyne modified silica cage and 1-azidoadamantane.
- Preparation of polymers having one and two azide or alkyne end-groups
- Preparation of nanocomposites by Huisgen 1,3-dipolar cycloaddition reaction between the silica cages and the polymers.

3. Results and Discussion

The preparation of hybrid polymers with defined structures containing spherosilicates or polyhedral oligomeric silsesquioxanes requires silica cages having alkyne or azide groups on all eight corners as well as polymers functionalized with one or two alkyne or azide groups.

The first part of this thesis deals with the preparation of modified silica cages, where the modification of spherosilicates and POSS are discussed in separate parts. In the second part details about the preparation of alkyne and azide modified polymers will be presented.

Before the combination of the prepared building blocks by Huisgen 1,3-dipolar cycloaddition reaction will be discussed, a chapter about the click reaction of alkyne modified spherosilicates with a model compound is included.

3.1 Synthesis of Alkyne and Azide modified Spherosilicates

3.1.1 Synthesis of $[Si_8O_{12}](Si(CH_3)_2CH_2Cl)_8$

The first step in the synthesis of modified spherosilicates is the preparation of tetramethylammonium silicate, octaanion $[Si_8O_{12}^{8-}]((CH_3)_4N^+)_8$ according to *Hoebbel et al.*[42] (Scheme 3.1.1). This initial hydrolysis/condensation step is described in detail in the introduction and is the same for the preparation of all spherosilicates in this thesis. The octaanion provided by this synthesis allows further functionalization with chlorosilanes as mentioned in the introduction.

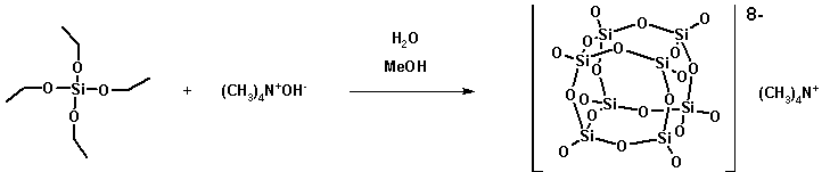

Scheme 3.1.1: Synthesis of Tetramethylammoniumsilicate, octaanion

The second step of the reaction was based on a literature known reaction[45] from which it differs slightly. Chloro(chloromethyl)dimethylsilane was dissolved in hexane and the octaanion was added dropwise resulting in a phase transfer reaction (Scheme 3.1.2).

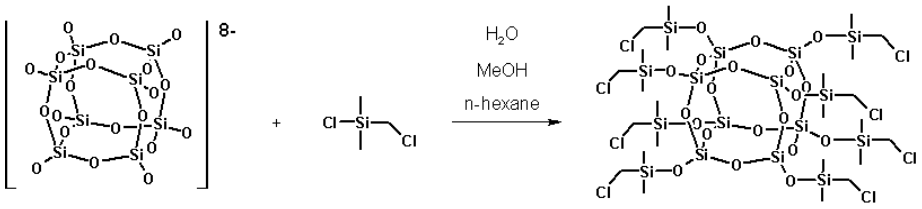

Scheme 3.1.2: Synthesis of $[Si_8O_{12}](Si(CH_3)_2CH_2Cl)_8$

The ^{1}H NMR analysis of the reaction products showed the presence of two sets of signals at 2.79/2.74 ppm and 0.29/0.21 ppm. The first set correlates with the σ methylene protons which connect the Si and the Cl atom, which is in concordance with earlier literature reports[45].

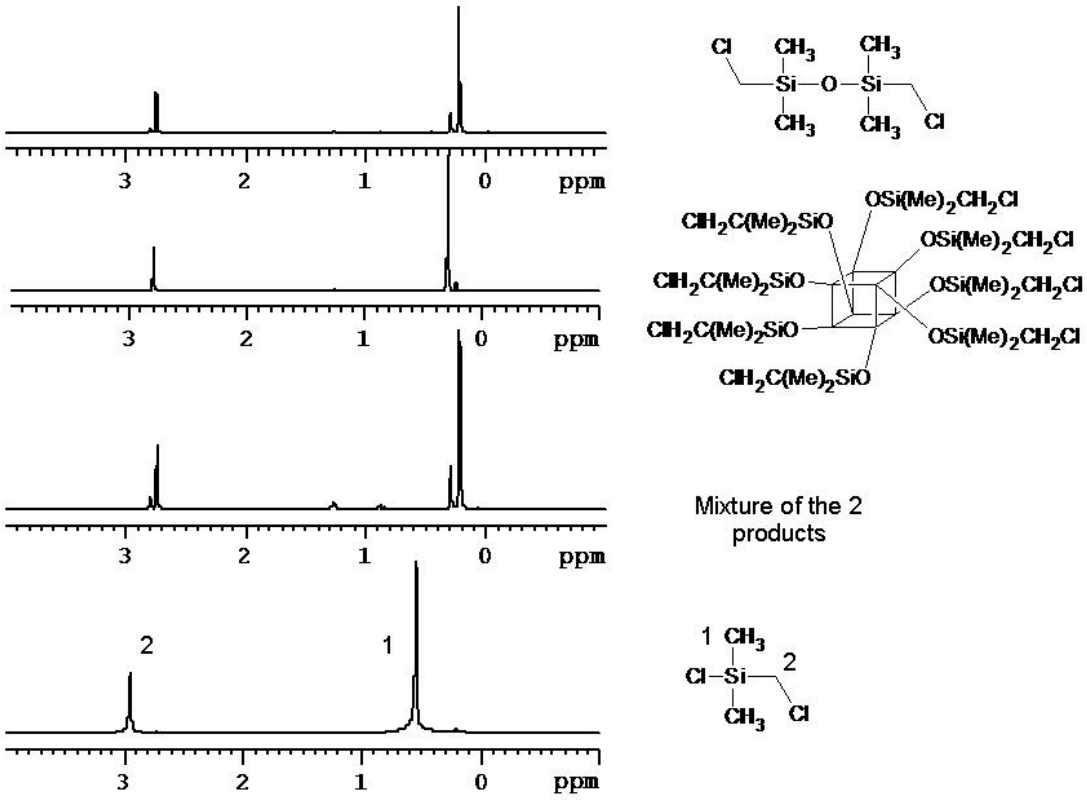

Figure 3.1.1: ^{1}H NMR spectra of the synthetic pathway for the production of the $Q_8M_8^{CH_2Cl}$

The second signal is assigned to the dimers of the chloromethyldimethylchlorosilane which are formed as byproducts during the synthesis. The ratio between the $Q_8M_8^{CH_2Cl}$ and the by-product could be increased by increasing the amount of chloromethyldimethylchlorosilane. An optimum yield was found for 3 equivalents excess per reactive anion corner. The by-products could be separated by the precipitation of the $Q_8M_8^{CH_2Cl}$ in methanol or its crystallization from acetonitrile. The final product was a white powder. ^{29}Si NMR measurements were carried out in order to prove the cage structure. A signal at -109.4 ppm (Figure 3.1.2) was detected, which correlates with the value in literature[45].

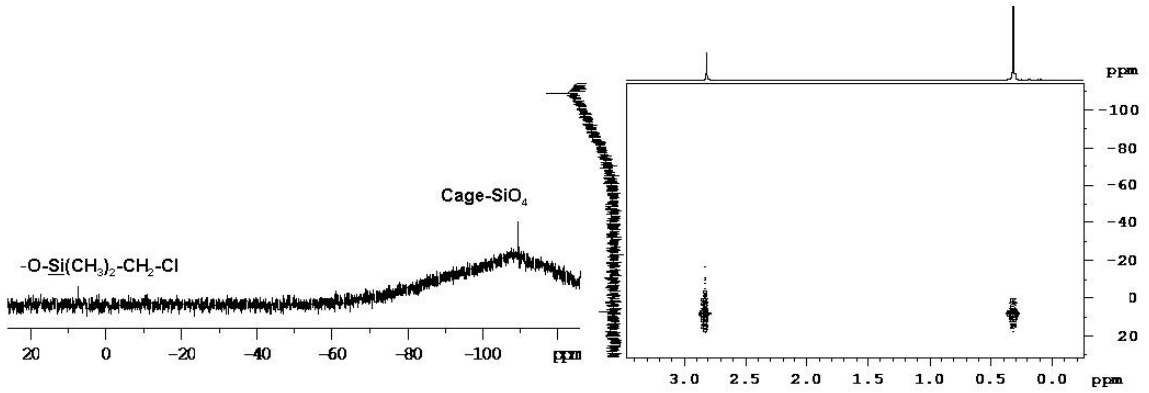

Figure 3.1.2: ^{29}Si NMR spectra (left) and Si-H HMBC spectra (right) of the Cl functionalized cage

Elemental analyses (Table 3.1) confirmed the successful synthesis by this simple pathway.

Sample	C (%)		H (%)		N (%)		Cl (%)	
	Exp.	Theo.	Exp	Theo	Exp	Theo	Exp	Theo
$Q_8M_8^{CH_2Cl}$	20.31	20.51	4.36	4.59	<0.05	-	19.75	20.18
$Q_8M_8^{CH_2Cl}$-cryst	20.81	20.51	4.31	4.59	0.3	-	19.72	20.18

Table 3.1: Elemental analysis of $Q_8M_8^{CH_2Cl}$

Synthesis of Alkyne-functionalized Spherosilicates:

Thus obtained chlorine substituted spherosilicate was reacted with ethinyl magnesiumbromide or sodium acetylide in order to get an alkyne substituted cage (Scheme 3.1.3).

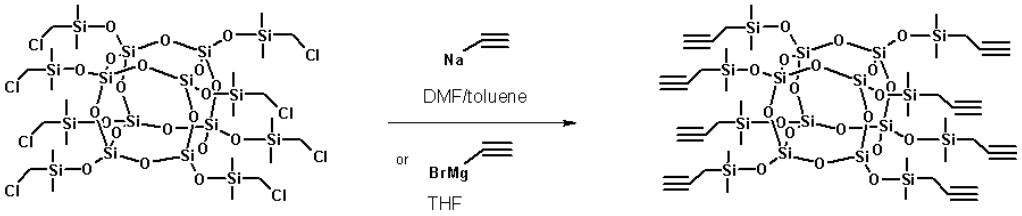

Scheme 3.1.3: Synthesis of alkyne modified spherosilicates

The reaction between sodium acetylide (18wt% slurry in xylene and mineral oil) and the chlorine-functionalized spherosilicate was carried out at room temperature in mixtures of toluene and DMF. The general pathway for the reaction is presented in Scheme 3.1.3. The reaction time was varying from one night up to 3 days. The products were characterized by various spectroscopic techniques such as FT-IR and NMR.

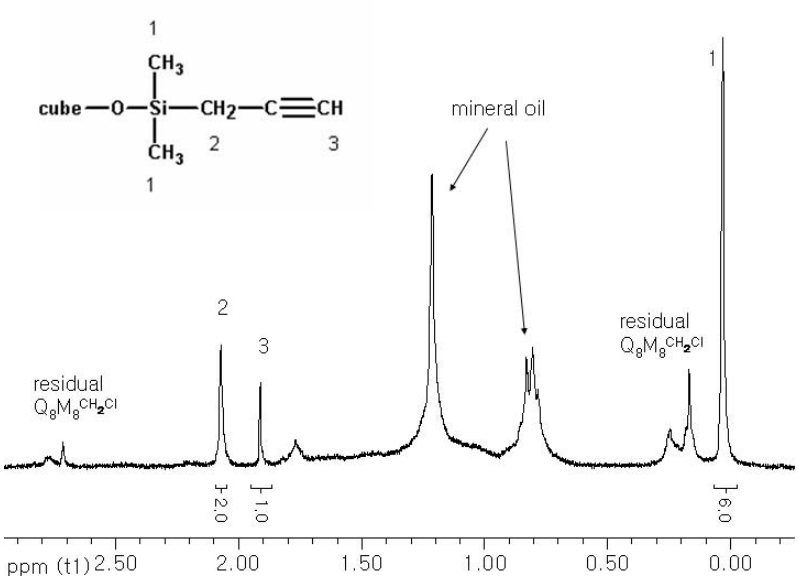

In the ^{1}H NMR of the reaction with sodium acetylide (Figure 3.1.3) the integration of the peaks corresponding to the ethinyl moieties is in very good agreement with the theoretical one ($CH:CH_2:Si(CH_3)_2$ = 1:2:6).

Figure 3.1.3: ^{1}H NMR of the reaction with sodium acetylide in CD_2Cl_2

The only drawback was the fact that even when employing a ratio of 1:4 between chlorine and sodium acetylide there still was some residual $Q_8M_8^{CH_2Cl}$ as seen from the Figure 3.1.3.

From the integration it appears that one third of the starting $Q_8M_8^{CH_2Cl}$ is not (fully) substituted. Further experiments at elevated temperature did not result in any significant improvement of the reaction yield. On the contrary, decomposition of the product was observed when the cage was heated for more than 3 days.

Due to the fact that the simple reaction between the $Q_8M_8^{CH_2Cl}$ and sodium acetylide was not satisfactory we tried another approach. Instead of using the sodium salt an ethinyl grignard reagent was used. The fully chlorine functionalized spherosilicate was dissolved in THF and added to a solution of ethinyl magnesiumbromide in the same solvent. The reaction mixture was heated to reflux for several hours.

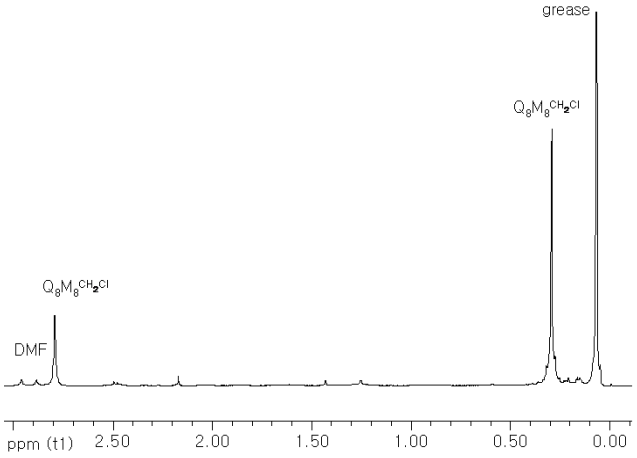

Figure 3.1.4: ^{1}H NMR of the reaction with ethinyl magnesiumbromide

The ^{1}H NMR (Figure 3.1.4) revealed that the reaction with ethinyl magnesiumbromide did not yield any alkyne modified spherosilicate at all.

Synthesis of Azide-functionalized Spherosilicates:

The fully chlorine substituted cages were reacted with sodium azide in a ratio of 1 to 1.15 (Cl : N_3) (Scheme 3.1.4). Functionalizing of only one corner of the cage was reported by *Binder et al.*[109] to be carried out with an excess of 5 equivalents of sodium azide at temperatures of 70ºC, overnight.

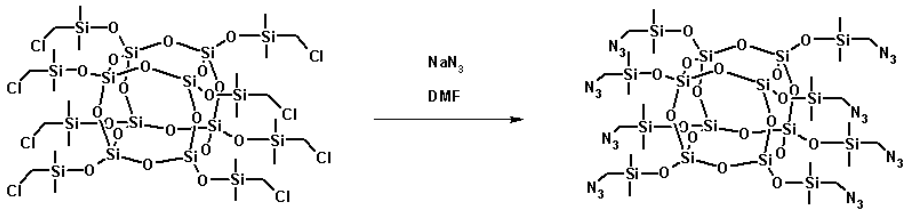

Scheme 3.1.4: Synthesis of azide modified spherosilicates

The reagents were stirred in a mixture of DMF and THF at 70°C. After 1 day a ^{1}H NMR (Figure 3.1.5) revealed no conversion.

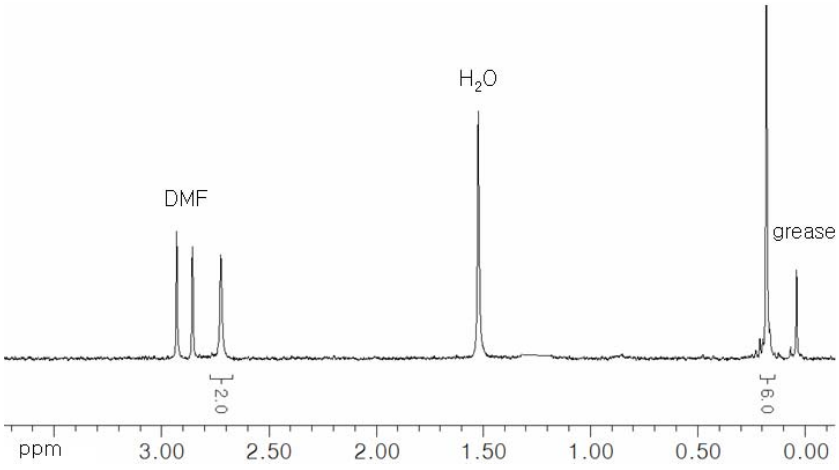

Figure 3.1.5: ^{1}H NMR of the reaction with sodium azide

The ^{1}H NMR of the reaction with sodium azide (Figure 3.1.5 - taken after 1 day) shows a new peak at 1.56 ppm, which is assigned to water. The signals at 2.72 ppm and 0.2 ppm correspond to $Q_8M_8^{CH_2Cl}$.

Even when a 4-fold excess of sodium azide was applied and stirred for three weeks at 70°C no azide modified spherosilicate could be obtained.

3.1.2 Synthesis of Bromine-modified Spherosilicate

The preliminary experiments described in part 3.1.1 of this thesis suggested that for the synthesis of spherosilicates having azide or alkyne groups at all eight corners a more reactive leaving group had to be provided. It is well known, that bromine is a better leaving group for S_N2 substitution reactions, than chlorine. For this reason, allyl bromide was hydrosilated with a spherosilicate having Si-H groups at all eight corners.

The reaction of $[Si_8O_{12}^{8-}]((CH_3)_4N^+)_8$ with chlorodimethylsilane in a phase-transfer reaction is literature known[110] and proceeds with high yields as it is shown in Scheme 3.1.5.

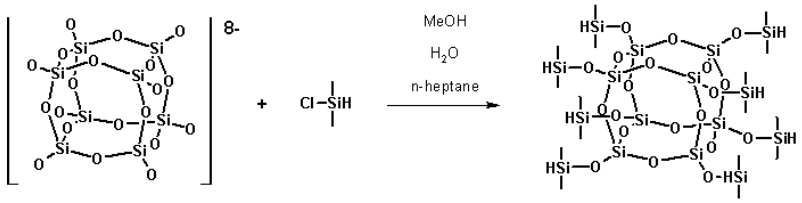

Scheme 3.1.5: Reaction of the octaanion with chlorodimethylsilane

Thus obtained $Q_8M_8^H$ was reacted with allyl bromide by a hydrosilation reaction as it is shown in Scheme 3.1.6 (in the following Schemes the spherosilicate cage will be shown as a cube in order to keep the spectators eye on the important side chains). The bromine end-group should enhance the reactivity towards the S_N2 substitution reaction with ethinyl magnesiumbromide and as well provide a good leaving group for the reaction with sodium azide.

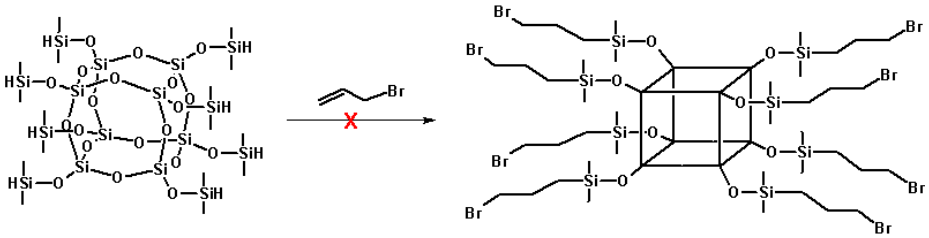

Scheme 3.1.6: Hydrosilation reaction of allyl bromide with Si-H substituted cage

The reaction was carried out using different catalysts and reaction temperatures. The reactions with Speier's catalyst according to *Provatas et al.*[111] were carried out in diethyl ether and DMF, while the reactions with Karstedt's catalyst required toluene as a solvent. Both reaction mixtures did not show any conversion after stirring for 24 hours at room

temperature. When heated to reflux, after two hours a white solid precipitated from the reaction mixtures. The ^{1}H NMR of the soluble compound shows only one large signal at 0.25 ppm, revealing that the hydrosilation reaction was not successful, but nevertheless the Si-H group disappeared. A ^{29}Si HMBC spectrum shows three differently shifted silicon atoms, all of them in the shift region of D units, long-range coupling with the protons at 0.25 ppm. A possible explanation for this result is that via bromination spherosilicates with Si-Br groups are formed. These groups are immediately hydrolysed and the resulting Si-OH groups condense, giving crosslinked products. Products with a low degree of crosslinking might be soluble and can be observed in the NMR spectra, while highly crosslinked cages are insoluble and thus the formation of a white precipitate can be explained.

Jankowiak et al.[112] observed similar reactions in the hydrosilation reaction of allyl chloride. They found, that the reaction of silanes with allyl chloride involves several processes (including chlorination), resulting in various different products, depending on the reaction conditions (Scheme 3.1.8).

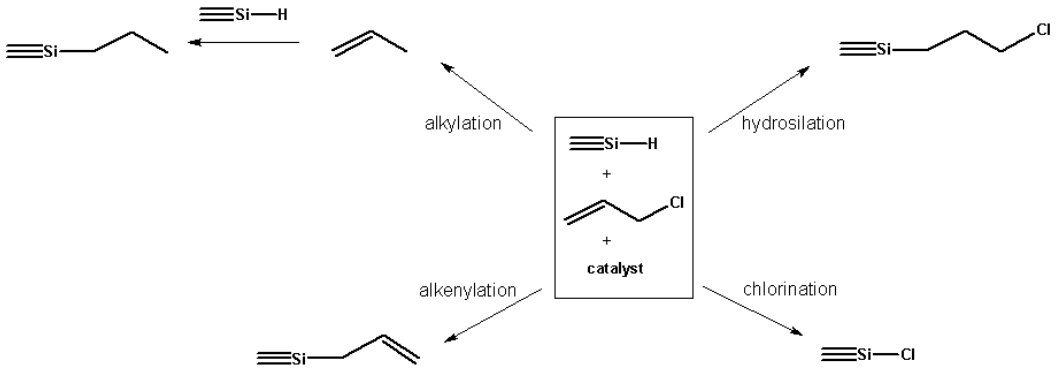

Scheme 3.1.8: Reaction pathways of hydrosiloxanes with allyl chloride

We believe that allyl bromide behaves more or less similar to allyl chloride and even if the product selectivity can be influenced by the reaction conditions, full eight corner hydrosilation reaction is supposed to be very unlikely (despite the results of *Provatas et al.*[111]).

3.1.3. Synthesis of Tosylate-modified Spherosilicate

It is difficult to obtain alkyl halogenide end-modified spherosilicates by other methods. Therefore a tosylate modified cage was targeted, which would also provide a good leaving group for nucleophilic substitution reactions. Thus, $Q_8M_8^H$ was modified with a hydroxy group by hydrosilation reaction with allyl alcohol (Scheme 3.1.9). The mechanism of hydrosilation reactions is explained in the introduction, but in hydrosilation reactions of allyl alcohol also Si-H alcoholysis, resulting in O-silylation, can occur. According to *Zhang and Laine*[113] the O-silylation can be suppressed applying high concentrations of Karstedt's catalyst and allyl alcohol.

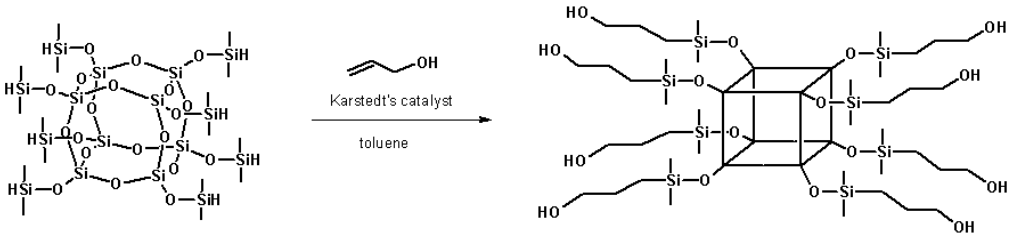

Scheme 3.1.9: Hydrosilation reaction of allyl alcohol with Si-H substituted cage

The hydrosilation reaction was carried out in toluene at room temperature and with an excess of allyl alcohol. The obtained product could be easily separated from the reaction mixture due to its immiscibility with toluene. The $Q_8M_8^{OH}$ could be obtained with high yields (90%) and was characterized by ^{1}H NMR, ^{13}C NMR, FT-IR-spectroscopy and SEC.

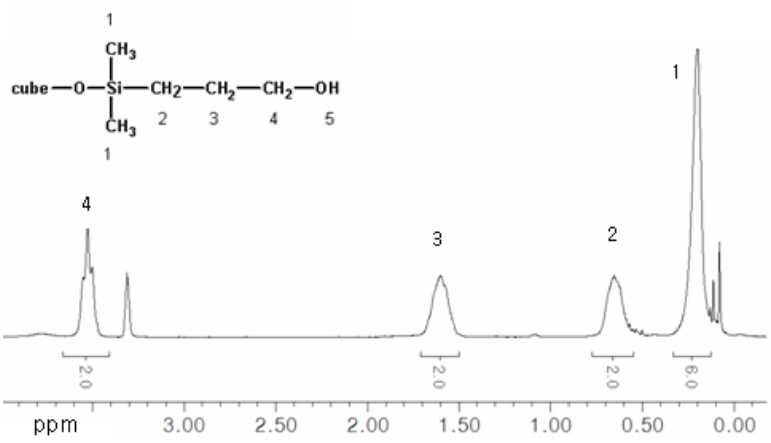

Figure 3.1.7: ^{1}H NMR and of $Q_8M_8^{OH}$

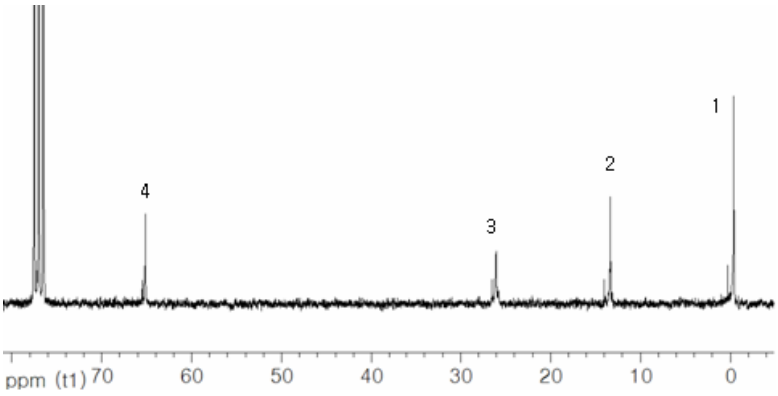

Figure 3.1.8: ^{13}C NMR of $Q_8M_8^{OH}$

The ^{1}H NMR (Figure 3.1.7) shows the hydroxypropyl group with the appropriate integration of the peaks. Nevertheless, the peaks in the ^{1}H NMR are rather broad and the expected multiplets cannot be seen, which led to the conclusion, that a small amount of by-product is formed, having nearly the same proton-shifts. In the ^{13}C NMR (Figure 3.1.8) small signals with shifts slightly differing from the carbons of the hydroxypropyl groups were observed. ^{1}H NMR and ^{13}C NMR show no peaks, that could be assigned to Si-O-CH_2-CH_2=CH_2 groups. Therefore, it is assumed, that C- and O-silylation occurred on the same side-chain, so that two cages are linked together. For this reason, the product was also characterized by SEC (Figure 3.1.9), which confirmed the presumption, that crosslinked by-products were formed by showing compounds with different molecular weights.

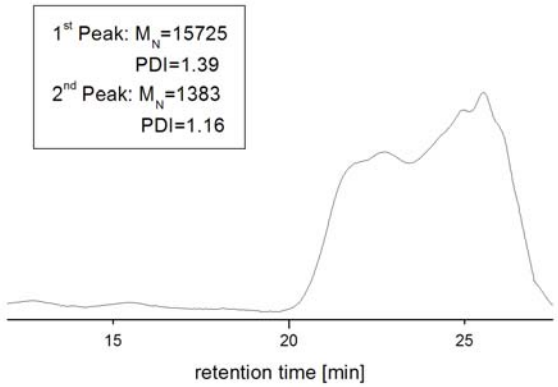

Figure 3.1.9: SEC plot of $Q_8M_8^{OH}$

The SEC plot confirms the conclusion drawn from the NMR spectra, that O- and C-silylation occur on the same chain, so that crosslinked products with higher molecular weights were formed.

Even though the linear polystyrene standards used for SEC have limited relevance for spherosilicates, the information that there are secondary products with considerably higher

molecular weights can be drawn from the SEC plot. The rather high polydispersity of the peaks leads to the conclusion, that different oligomers are formed. The maximum at a molecular weight of about 15700 shows that oligomers with about ten spherosilicate units are favoured. Even if in the NMR spectra only small amounts of crosslinked chains were observed, the first peak in the SEC plot – which is assigned to crosslinked cages – is only slightly smaller than the second peak. Regarding that one cage has 8 corners and thus one out of sixteen corners is enough to have two cages crosslinked these observations are plausible.

One explanation for the unsuccessful reaction is that O-silylation occurred due to the fact that the Karstedt's catalyst used was already old and partly decomposed, because the use of higher concentrations of catalyst and allyl alcohol did not reduce the amount of O-silylated by-products as it should according to *Zhang and Laine*[113].

Even though $Q_8M_8^{OH}$ could not be obtained pure, but with a crosslinked by-product, the OH groups were tosylated without any further purification. Thus, the obtained $Q_8M_8^{OH}$ was allowed to react with p-toluenesulfonylchloride in the presence of triethylamine and dimethylaminopyridine as a catalyst (Scheme 3.1.10) in dichloromethane. The reaction mixture was stirred for 24 hours at room temperature and the pure product could be obtained by column chromatography.

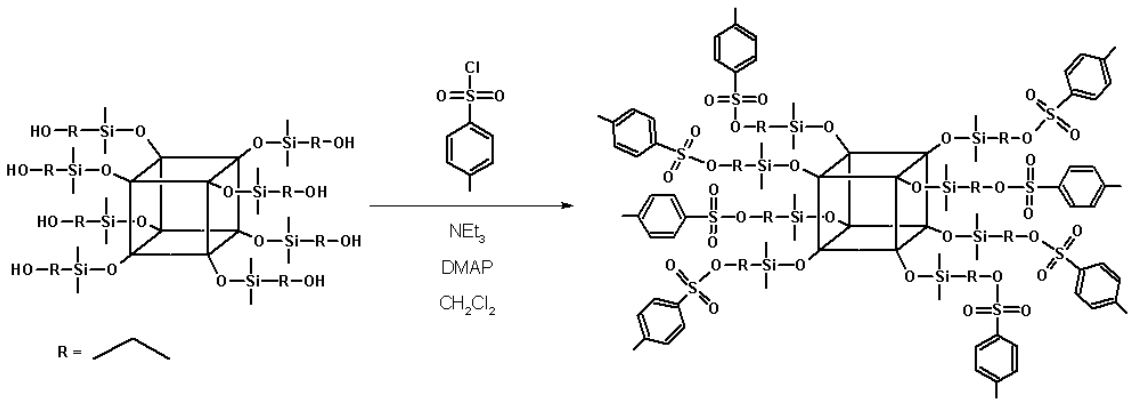

Scheme 3.1.10: Synthesis of $Q_8M_8^{OTos}$

The product was characterized by ^{1}H NMR, ^{13}C NMR, ^{29}Si NMR, FT-IR and SEC. The ^{1}H NMR and the ^{13}C NMR (Figure 3.1.10) show the tosylate modified cage as it was obtained after column chromatography.

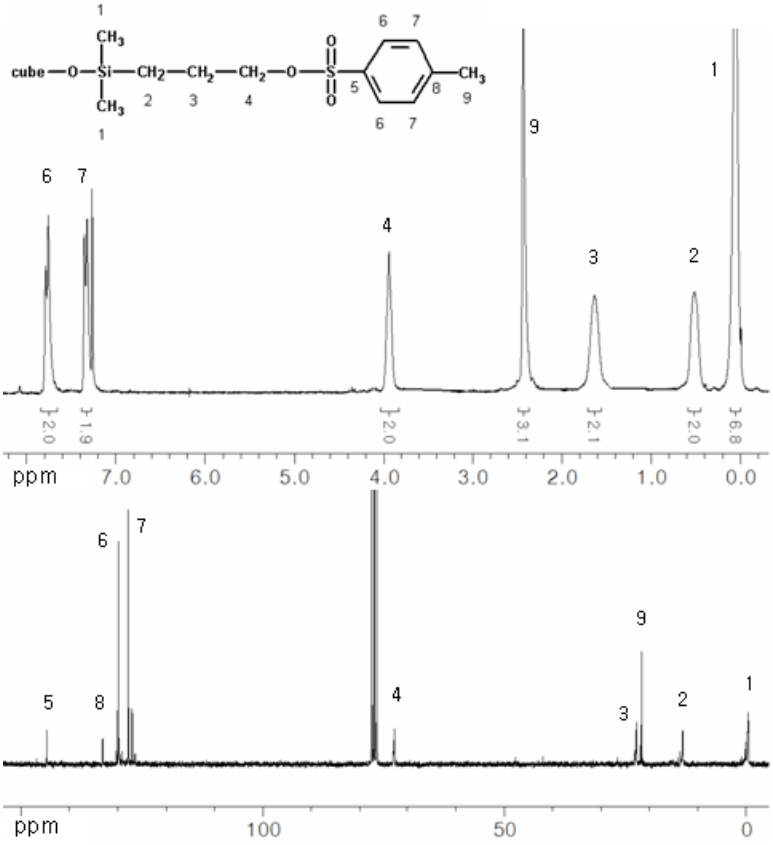

Figure 3.1.10: ^{1}H NMR (up) and ^{13}C NMR (down) of $Q_8M_8^{OTos}$

The peaks can be assigned to the corresponding structural elements by their numbers. Again, in the NMR spectra no by-products were observed, but as discussed for $Q_8M_8^{OH}$, 5% of crosslinking chains are enough to have nearly half of the cages crosslinked. For this reason, SEC measurements were carried out in order to detect crosslinked cages.

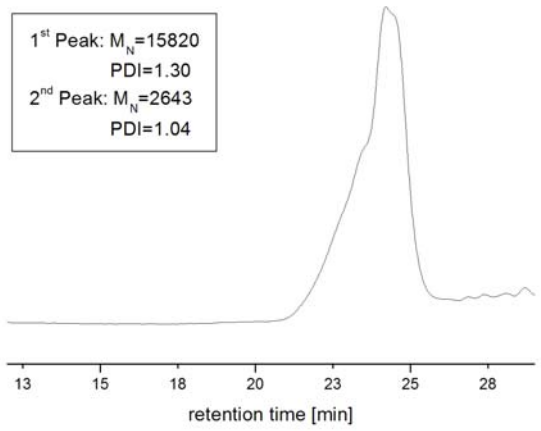

Figure 3.1.11: SEC plot of $Q_8M_8^{OTos}$

For the tosylate modified spherosilicate the amount of crosslinked cages (SEC plot Figure 3.1.11) seems to be considerably smaller than for $Q_8M_8^{OH}$ (Figure 3.1.9), which means, that it could be reduced (most probably by column chromatography). Unfortunately, not all the crosslinked cages could be removed.

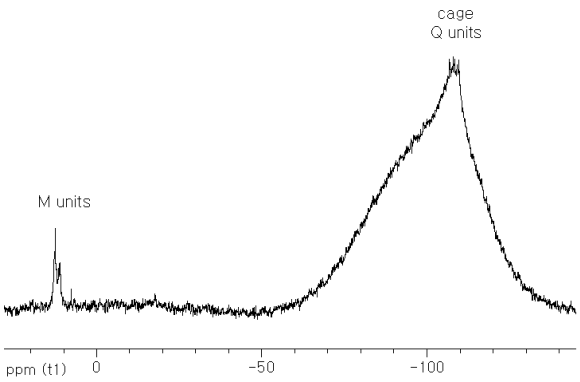

The ^{29}Si-NMR does not show one sharp peak at -108 ppm, but various small peaks around this value, which is due to an influence of crosslinked corners on the silicon atoms of the cage. The signal for the Q units cannot be clearly distinguished from the glass peak.

Figure 3.1.12: ^{29}Si NMR of $Q_8M_8^{OTos}$

Moreover, ^{29}Si NMR reveals two peaks for M units at 11.2 and 12.5 ppm. A peak for D units formed by O-silylation cannot be seen, because the amount of O-silylated chains is too small.

Synthesis of Azide-modified Spherosilicate:

The small amount of crosslinked cages, which are still in the nanometer size regime, does not influence the properties of a potential hybrid material. Thus, the obtained tosylate-modified spherosilicate was used for the preparation of azide-modified cages.

The tosylate-modified spherosilicate was reacted with sodium azide (Scheme 3.1.11) in order to obtain stable spherosilicates with azide-groups on all eight corners. The reaction was carried out in dry DMF with an excess of sodium azide by stirring for 18 hours at 40°C. After this time a ^{1}H NMR revealed that 15% of the corners did not react and thus the reaction temperature was elevated to 60°C for 24 hours.

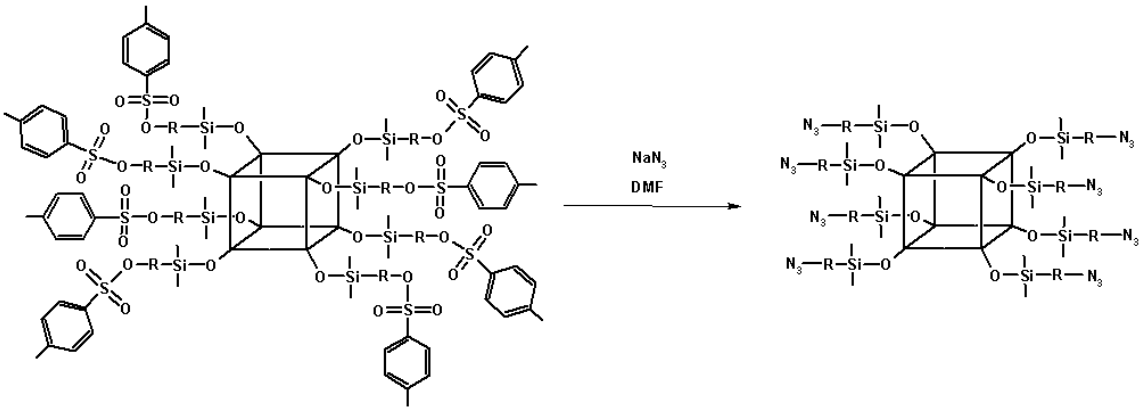

Scheme 3.1.11: Reaction of $Q_8M_8^{OTos}$ with sodium azide

The tosylate-modified corners could be reduced to less than 1% as observed in ^{1}H NMR (Figure 3.1.13).

The eight-corner azide modified spherosilicate was characterized by ^{1}H NMR, ^{13}C NMR, ^{29}Si NMR and FT-IR.

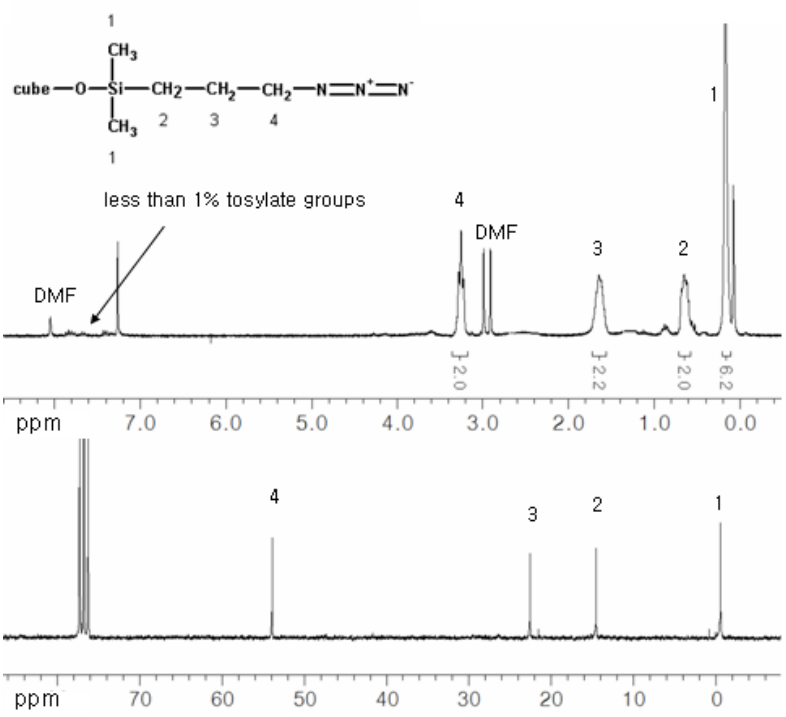

Figure 3.1.13: ^{1}H NMR (up) and ^{13}C NMR (down) of $Q_8M_8^{azide}$

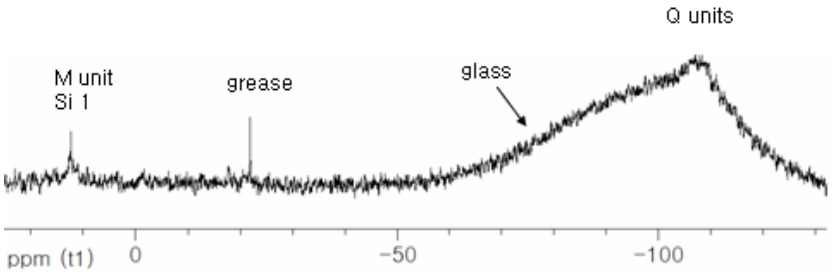

Figure 3.1.14: ^{29}Si NMR of $Q_8M_8^{azide}$

The ^{1}H NMR (Figure 3.1.13) shows the disappearance of almost all aromatic protons and thus proves the full conversion and consequently the eight corner azide functionalization of the spherosilicate. The new peak at 54 ppm in the ^{13}C NMR (Figure 3.1.13) is assigned to the carbon bonded to the azide. The only drawback was, that it was not possible to give the prove that the cage is still intact by ^{29}Si NMR (Figure 3.1.14), because it does not show one sharp peak at -108 ppm for the Q units but various indiscrete peaks around this value (which cannot be clearly distinguished from the glass-signal). This observation was already explained for the tosylate modified spherosilicate and is due to the interactions between differently substituted chains (due to O-silylation and a small amount of tosylate groups).

Thus, the substitution reaction with sodium azide was successful with full conversion and gave a stable product that could be obtained with high purity and did not require any further purification.

Synthesis of Alkyne-modified Spherosilicates:

Various attempts to convert the tosylate- into alkyne-groups by reaction with sodium acetylide or ethinyl magnesiumbromide failed.

The substitution reaction with sodium acetylide was carried out at room temperature in DMSO or mixtures of DMF and THF. The general pathway for the reaction is presented in Scheme 3.1.12.

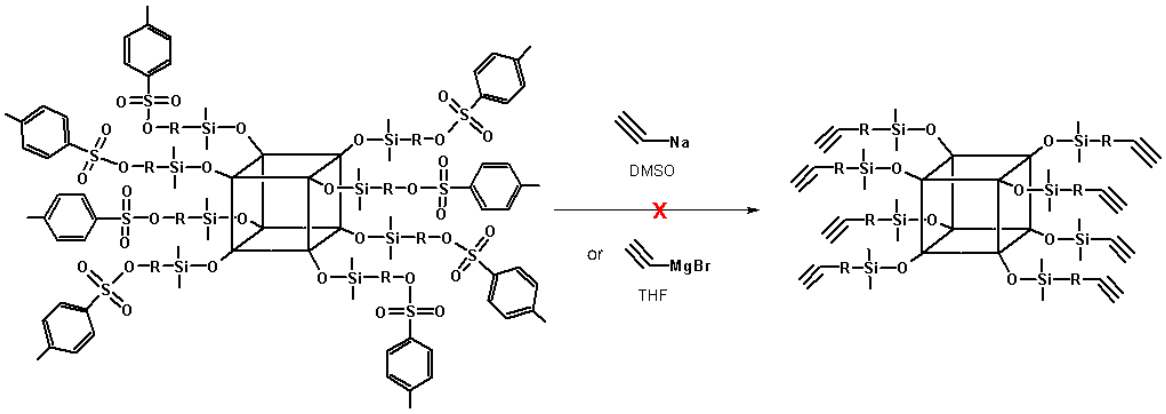

Scheme 3.1.12: Reaction of $Q_8M_8^{OTos}$ with sodium acetylide and ethinyl magnesiumbromide

The ^{1}H NMR (Figure 3.1.15) shows peaks that can be assigned to a hydroxypropyl modified spherosilicate. The HSQC and HMBC spectra confirm this suggestion drawn from the ^{1}H NMR.

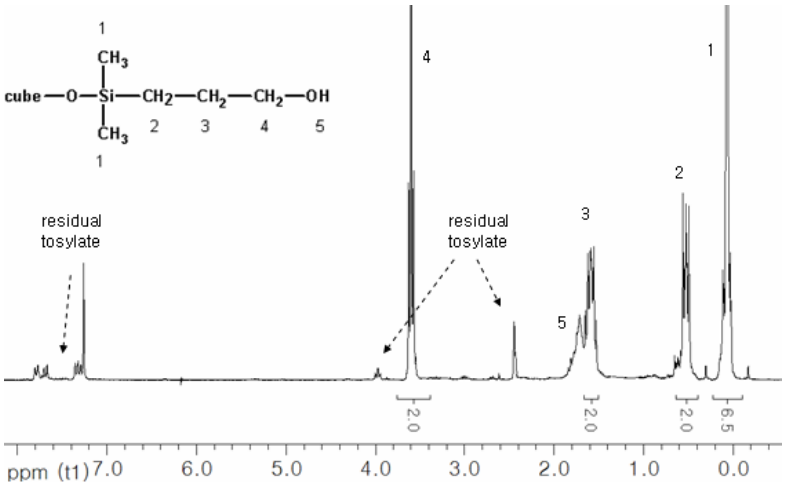

The ^{1}H NMR shows peaks with the same shifts as found earlier for the spherosilicate with hydroxypropyl groups.

Figure 3.1.15: ^{1}H NMR of the reaction with sodium acetylide

Obviously, the tosylate is hydrolyzed. According to *Nummert et al.*[114] the electrophilic solvating power of the solvent is the main factor in the hydrolysis of tosylates. Unfortunately, for this reaction a solvent with a high solvating power is required to dissolve the sodium acetylide.

Due to the fact, that the reaction with sodium acetylide was not satisfactory, another approach using an ethinyl grignard reagent was used. The tosylate modified spherosilicate was dissolved in dry THF and ethinyl magnesiumbromide was added. After stirring 24 hours at room temperature a sample was taken and the ^{1}H NMR revealed no reaction. Thus, the reaction mixture was heated to reflux and after 24 hours a new peak at 1.8 ppm

was formed – indicating the formation of alkyne substituted chains – and the peaks in the aromatic region belonging to the tosylate were considerably smaller (Figure 3.1.16). The tosylate was completely removed after another 48 hours of reflux (Figure 3.1.16). However, the protons of the CH_2 group next to the ethinyl moiety should be found around 2 ppm, but as the peak at 3.9 ppm is diminishing a new one is arising at 3.4 ppm.

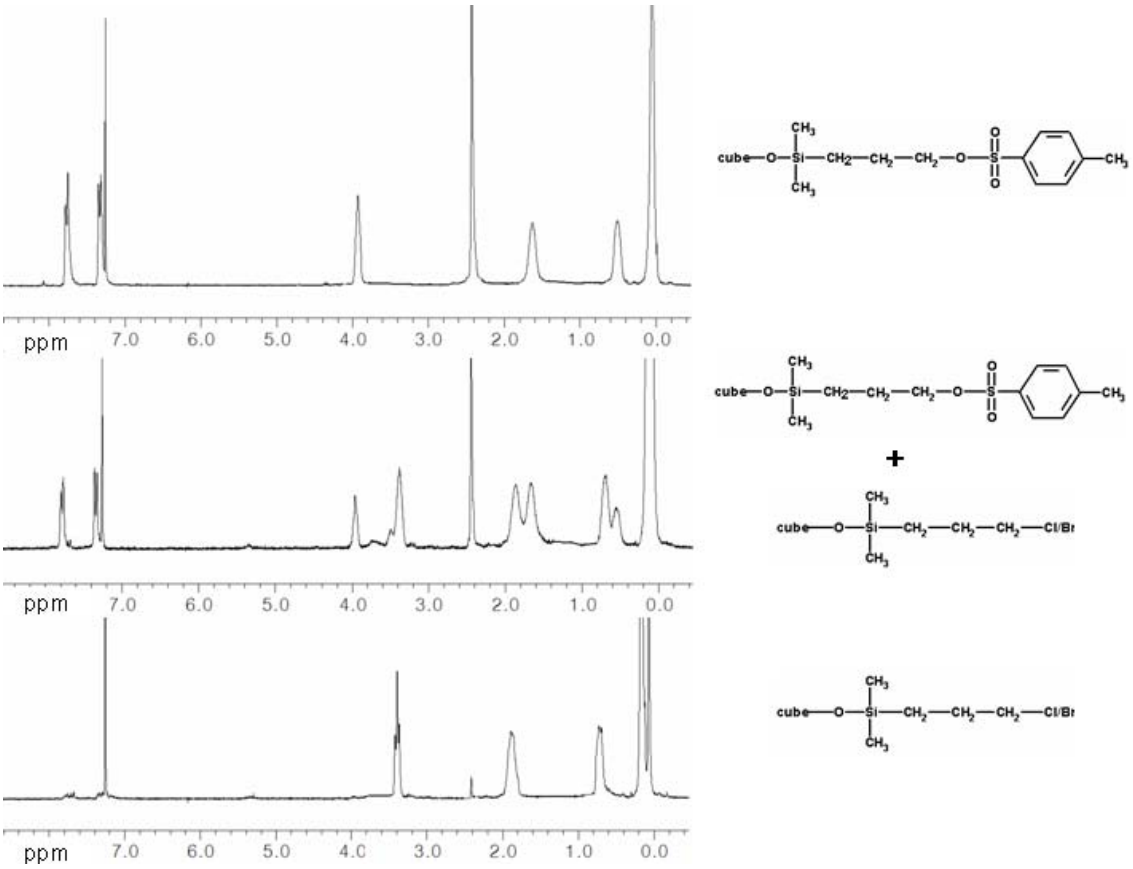

Figure 3.1.16: ^{1}H NMR of the reaction with ethinyl magnesiumbromide after different reaction times

Also the HSQC spectrum (Figure 3.1.17, after full conversion) shows no alkyne peak in the carbon-region around 90 ppm, but a peak at 37 ppm, which couples with protons at 3.4 ppm. This signal cannot be attributed to any possible structure, but a halogen end-modified chain. The H,H-COSY spectrum shows coupling of the protons at 1.8 ppm with 3.4 and 0.7 ppm, which – regarding also the shifts in the HSQC – allows the assumption, that the chain of three carbons is end-functionalized with a halogen, most likely chlorine. A possible explanation for this observation is that the tosylate is removed during the reaction and some instable intermediate is formed, which decomposes forming a C-Cl bond when the product is washed with NH_4Cl and brine after the reaction. Up to now, the

author has not been able to elucidate the structure of the intermediate, but it is assumed that a carbeniumion is formed, stabilized by interaction with TosMgBrCCH$^-$.

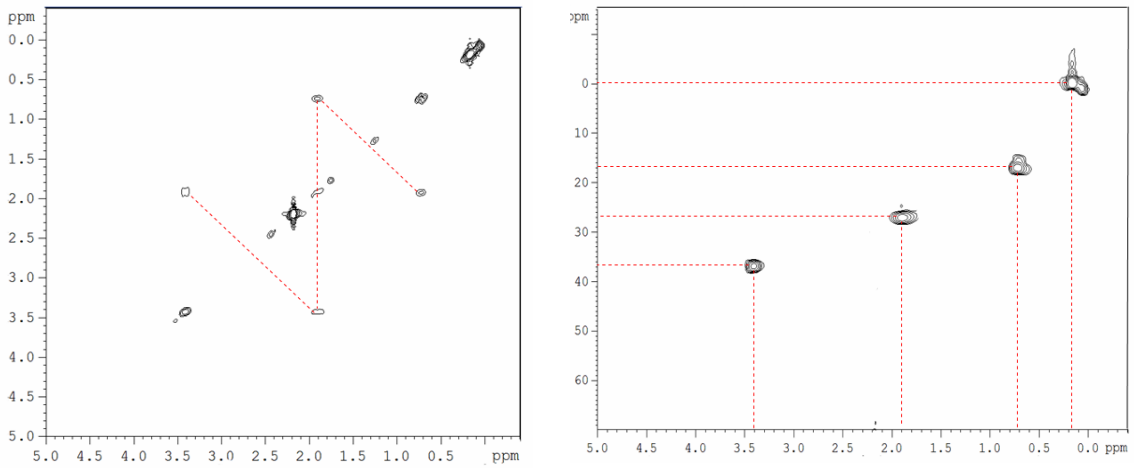

Figure 3.1.17: H,H COSY (left) and HSQC (right) spectra of the reaction with ethinyl magnesiumbromide

3.1.4 Synthesis of Chlorine-modified Spherosilicate

The previously described methods showed that for the preparation of alkyne modified spherosilicates a new pathway had to be searched. A more reactive species for the nucleophilic substitution reaction with ethinyl magnesiumbromide was required to obtain full eight corner functionalized cages. The Si-Cl bond would be a suitable group for the nucleophilic substitution reaction with ethinyl magnesiumbromide, because it is very reactive. Unfortunately, dichlorodimethylsilane does not selectively react with one chloro group when reacted with the octaanion, but forms a network of spherosilicate cages[115]. For this reason spherosilicates bearing Si-Cl bonds were prepared by a procedure reported by *Jutzi et al.*[116].

The first step of this synthesis sequence was again the hydrolysis/condensation reaction of tetraethoxysilane as it was described before. The chlorosilane used for the subsequent functionalization of the spherosilicate provided a vinyl group[45] (Scheme 3.1.13).

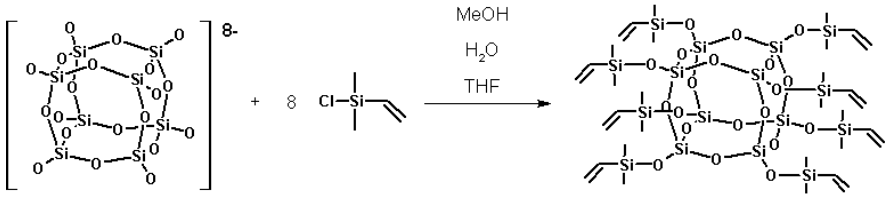

Scheme 3.1.13: Functionalization of spherosilicate with chlorodimethylvinylsilane

$Q_8M_8^{vinyl}$ could be obtained as a white solid in high yields and easily be separated from cages with unreacted corners by washing with methanol.

The vinyl groups of the spherosilicate could be converted into Si-Cl bonds by hydrosilation reaction with chlorodimethylsilane[116] (Scheme 3.1.14) using Karstedt's catalyst.

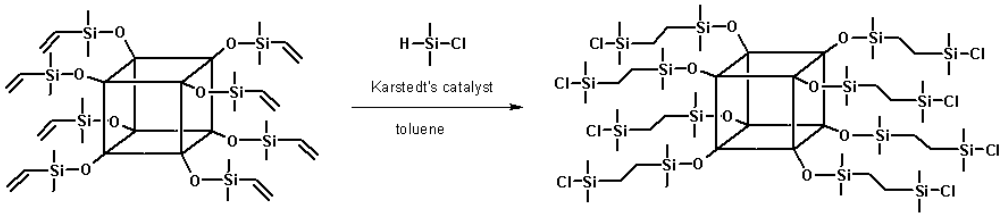

Scheme 3.1.14: Hydrosilation reaction of $Q_8M_8^{vinyl}$ with chlorodimethylsilane

The reaction was carried out in dry toluene with an excess of chlorodimethylsilane. The catalyst was removed by filtration over silica gel and no further purification was required. The product was characterized by ^{1}H NMR, ^{13}C NMR and FT-IR spectroscopy.

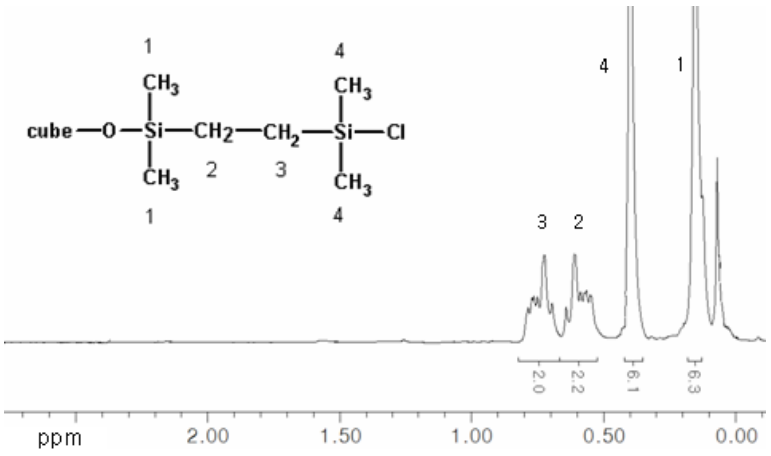

Figure 3.1.18: ^{1}H NMR of $Q_8M_8^{Cl}$

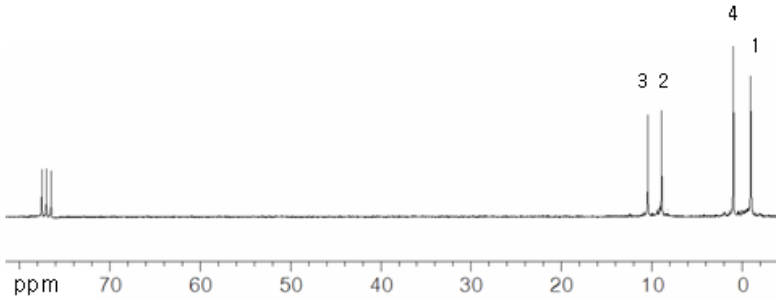

Figure 3.1.19: ^{13}C NMR of $Q_8M_8^{Cl}$

The ^{1}H NMR (Figure 3.1.18) reveals that the CH_2 groups give rather broad peaks, this might be due to the influence of a small amount of β-silation or non-silylated corners, which cannot be observed in the NMR spectra but influences the neighbouring CH_2 groups[116]. Nevertheless the ^{13}C NMR (Figure 3.1.19) shows explicitly the different CH_2 and CH_3 groups and no contamination.

Subsequently the chlorine-modified cage was used for the nucleophilic substitution reaction with ethinyl magnesiumbromide (Scheme 3.1.15).

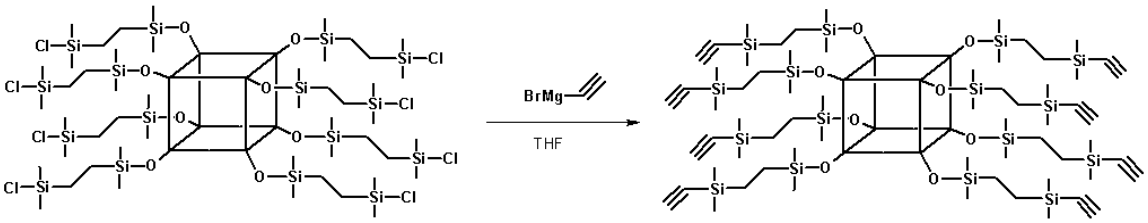

Scheme 3.1.15: Substitution reaction of $Q_8M_8^{Cl}$ with ethinyl magnesiumbromide

$Q_8M_8^{Cl}$ was stirred with ethinyl magnesiumbromide in dry THF at 40°C for 4 hours and the excess ethinyl magnesiumbromide was removed by washing with water and saturated aqueous NaCl solution.

The product was obtained in high yields (74%) and characterized by ^{1}H NMR, ^{13}C NMR, ^{29}Si NMR and FT-IR spectroscopy.

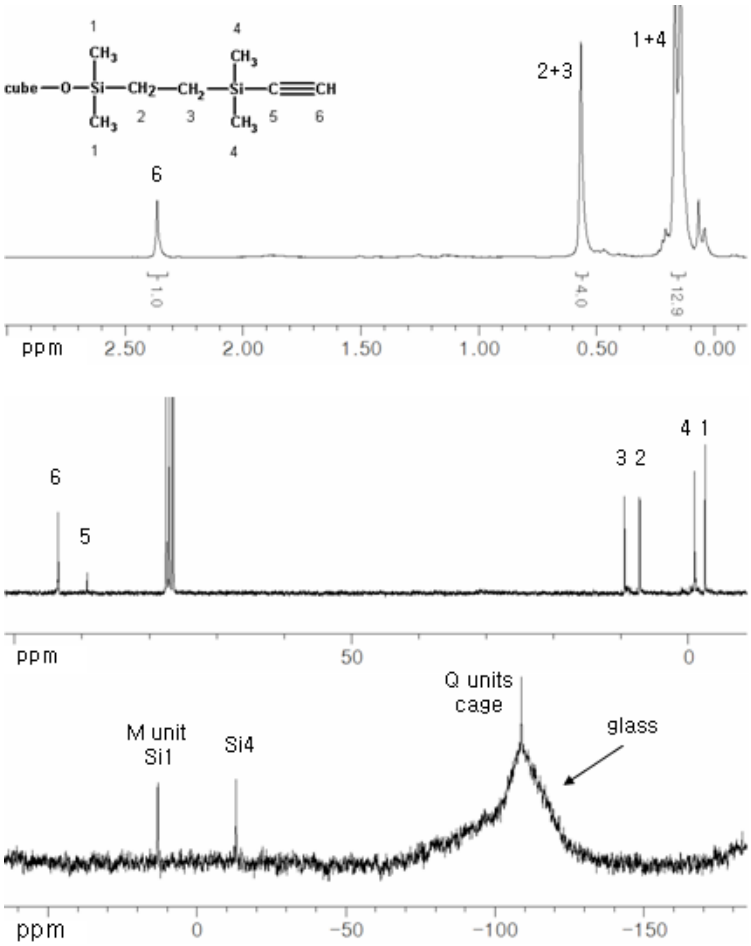

Figure 3.1.20: ^{1}H NMR (up), ^{13}C NMR (middle) and ^{29}Si NMR (down) of $Q_8M_8^{alkyne}$

As observed in the ^{1}H NMR in Figure 3.1.20, the only considerable contamination is grease (small peak at 0.067 ppm), which is chemically inert and does not affect the success of the Huisgen 1,3-dipolar cycloaddition reaction. Thus, for the use in the click reaction it did not require any further purification. The ^{13}C NMR (Figure 3.1.20) shows the characteristic shifts of the alkyne carbons at 89 and 93 ppm and in the ^{1}H NMR the terminal proton of the alkyne can be seen at a typical shift of about 2.4 ppm. The broad peaks of the CH_2 groups of the chlorine modified cage (Figure 3.1.18) are fully disappeared. Moreover, as the product has been washed with water, residual chlorine-modified cage would have been hydrolysed and the OH-modified cage would be observed in ^{29}Si NMR as a T unit (about 70 ppm). The prove that the cage is still intact is given by ^{29}Si NMR with a sharp and single peak at -108.8 ppm, corresponding to the quaternary Si units.

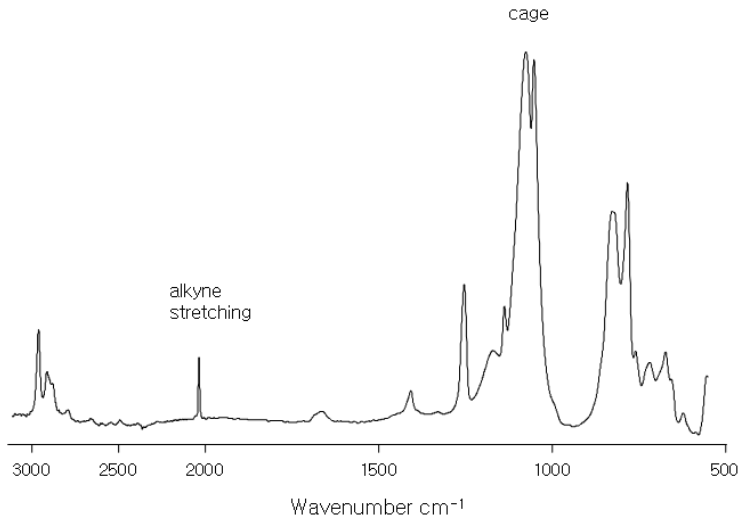

The typical alkyne stretching vibration is observed at 2035 cm^{-1} in the FT-IR (Figure 3.1.21).

Figure 3.1.21: FT-IR of $Q_8M_8^{alkyne}$

3.2. Synthesis of Alkyne-modified POSS

The difference between spherosilicates and POSS and the main approaches for their synthesis are explained in the introduction. Due to the possibility of the synthesis of alkyne modified trialkoxysilanes and the direct condensation thereof, POSS systems seemed to be more promising for the introduction of functional groups on all eight corners than spherosilicates.

3.2.1. Condensation of Ethinyltriethoxysilane

The most versatile and effective way to functionalized POSS cages is the hydrolysis and condensation reaction of organically modified trialkoxysilanes in presence of an accelerating agent, as discussed in the introduction. Thus, the first approach to eight corner alkyne modified POSS was the condensation of ethinyltriethoxysilane. The method used was related to the synthesis of the vinyl modified POSS reported by *Bassindale et al.*[53]. It is based on the reaction of chlorotriethoxysilane with ethinyl magnesiumbromide following a literature known procedure[117] (Scheme 3.2.1).

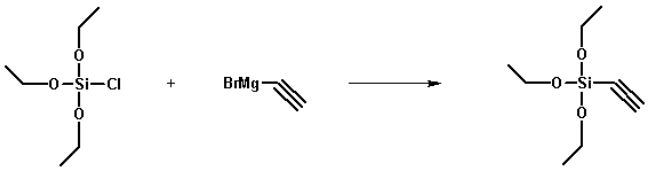

Scheme 3.2.1: Preparation of Ethinyltriethoxysilane

The reaction was carried out in dry THF at room temperature with an excess of ethinyl magnesiumbromide. The excess ethinyl magnesiumbromide and the by-products were removed by washing with water and saturated NaCl solution. The pure product was characterized by ^{1}H NMR, ^{13}C NMR and FT-IR.

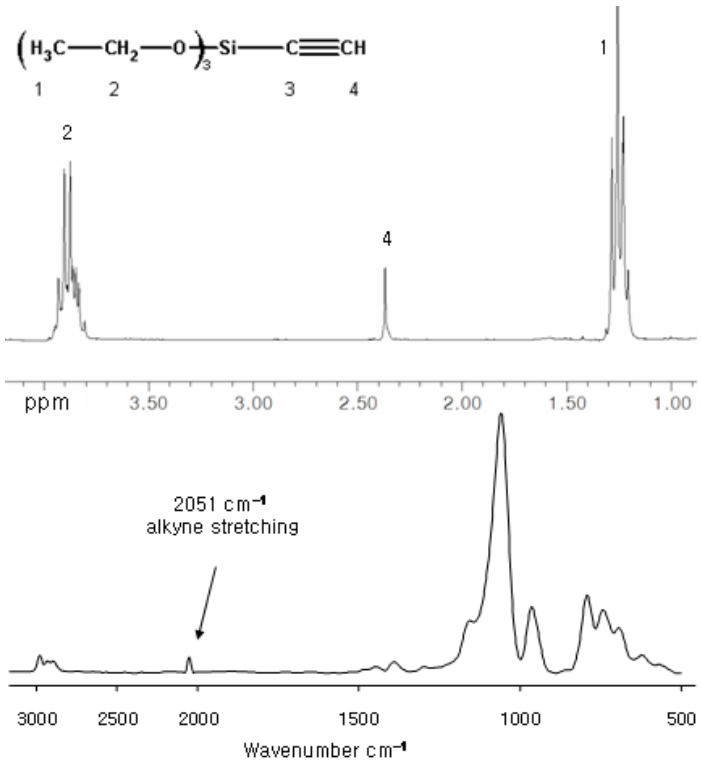

Figure 3.2.1: ^{1}H NMR (up) and FT-IR (down) of Ethinyltriethoxysilane

The ^{1}H NMR in Figure 3.2.1 shows the alkyne peak at the typical shift of 2.4 ppm and the quadruplet and triplet of the ethoxy groups at 3.9 ppm and 1.3 ppm. In the FT-IR (Figure 3.2.1) spectrum the characteristic alkyne stretching vibration is observed at 2051 cm^{-1}.

The hydrolysis and condensation reaction for the preparation of the alkyne-modified POSS was carried out following the procedure reported by *Bassindale et al.*[53] for the hydrolysis/condensation of vinyltriethoxysilane (Scheme 3.2.2). As mentioned in the

introduction, TBAF is an accelerating agent for the hydrolysis/condensation reaction of silicon alkoxides and reduces the reaction time from several months to 24 hours. The reaction was carried out in toluene using a ratio of ethinyltriethoxysilane/TBAF of 3/1.

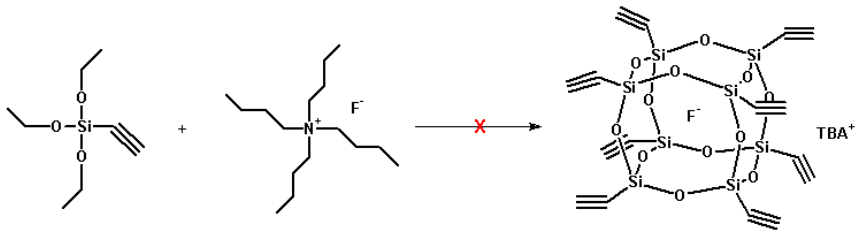

Scheme 3.2.2: Hydrolysis/Condensation of Ethinyltriethoxysilane

During the reaction a white solid precipitated from the reaction mixture, which was analyzed by FT-IR, while the solution was characterized by ^{1}H NMR, ^{13}C NMR and FT-IR.

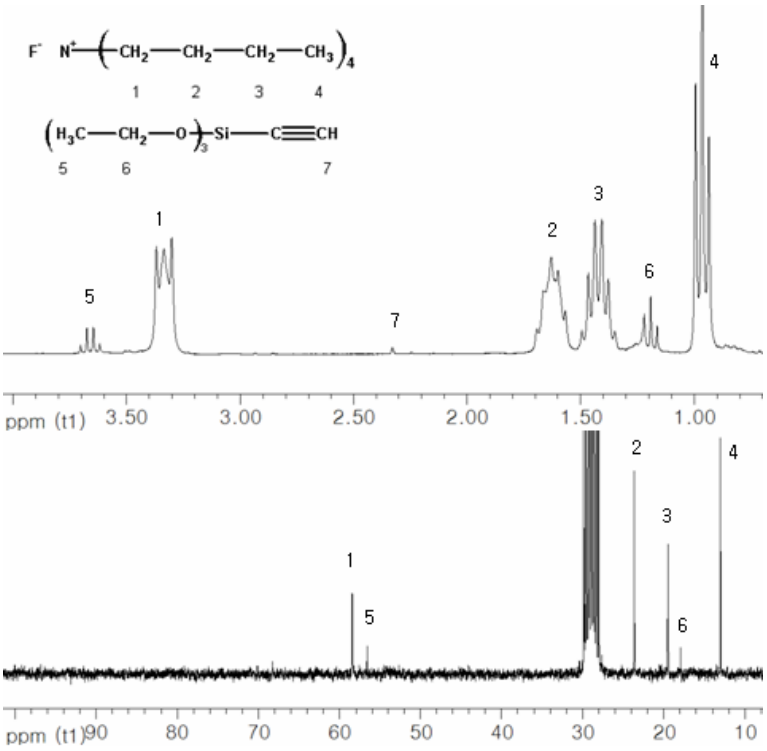

Figure 3.2.2: ^{1}H NMR (up) and ^{13}C NMR (down) of the condensation of acetyltriethoxysilane

The ^{1}H NMR (Figure 3.2.2) and the ^{13}C NMR (Figure 3.2.2) spectra of the soluble part show TBAF and some leftover ethoxy groups, that were not hydrolysed, but no alkyne group, which should be shifted to ~2.4 ppm in the ^{1}H NMR and to 89 and 93 ppm in the ^{13}C NMR. Neither the FT-IR spectrum (Figure 3.2.3) of the white solid, nor the one of the

soluble compound show absorption in the region of the alkyne stretching vibration (around 2000-2100 cm^{-1}).

In the FT-IR spectrum of the insoluble part a broad peak around 1000 cm^{-1} is observed, which is assigned to the Si-O and Si-C vibrations of the newly formed silica network. The strong peak at about 2360 cm^{-1} is due to CO_2 and an artefact of the ATR method.

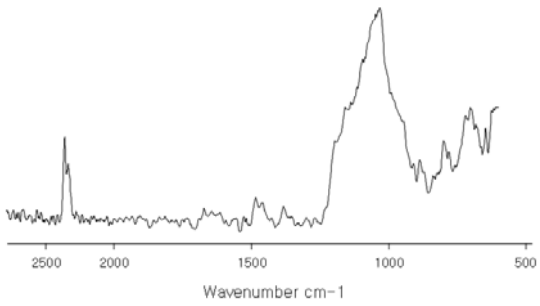

Figure 3.2.3: FT-IR of the precipitate from the condensation of Ethinyltriethoxysilane

An explanation for these results is that the hydrolysis/condensation was not controlled, and thus a crosslinked silica network was obtained. The reason for this uncontrolled reaction process is most probably that the TBAF reacts in another way with the alkyne.

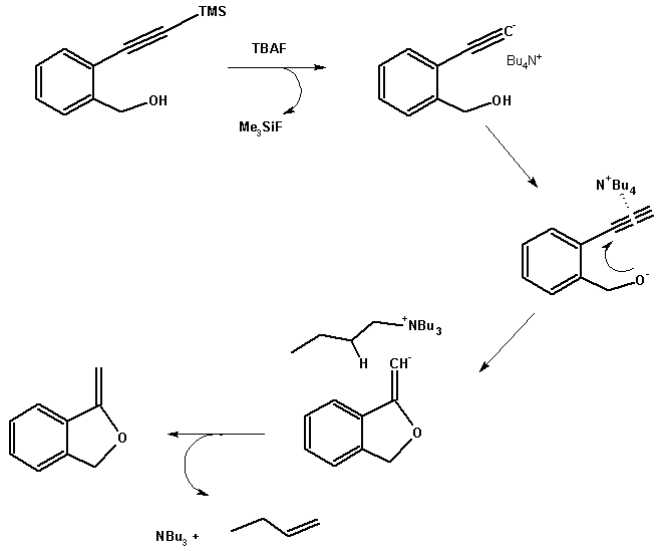

Scheme 3.2.3: Possible mechanism for the attack of TBAF on triplebonds

According to *Hiroya et al.*[118], TBA^+ coordinates to triplebonds, activating them for an attack of a hydroxy group in the surrounding. They propose the mechanism shown in Scheme 3.2.3 for TBAF-catalyzed cyclization reactions.

The reaction course proposed by *Hiroya et al.* is excluded for the reaction of ethinyltriethoxysilane with TBAF, because otherwise the ^1H NMR and ^{13}C NMR would show tributylamine and butene. Nevertheless, we suppose that TBA^+ coordinates to the triplebond releasing HF, thus removing the fluoride ion which is needed for a controlled

hydrolysis and condensation reaction[119]. Unfortunately, we were not able to find out what occurred with the triplebond, but it is definitely destroyed.

3.2.2. Synthesis of Chlorine modified POSS

The second approach was carried out according to the formation of functionalized spherosilicates. It has the advantage that the eight corner chlorine functionalized POSS cage was commercially available. Thus, the alkyne POSS cage could be obtained easily by a one-step reaction via substitution with ethinyl magnesiumbromide (Scheme 3.2.4). The chlorine modified POSS was dissolved in dry THF and after addition of ethinyl magnesiumbromide the solution was heated to 40°C for 3 hours.

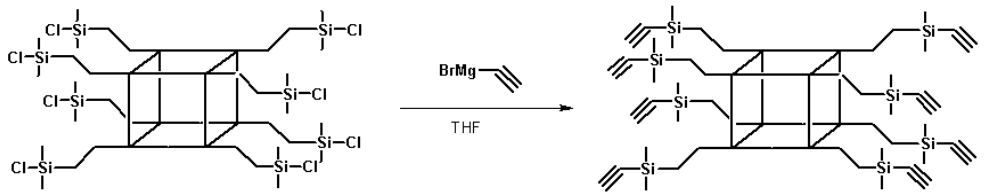

Scheme 3.2.4: Substitution reaction of POSS^{Cl} with ethinyl magnesiumbromide

The eight corner alkyne modified POSS was characterized by ^{1}H-NMR, ^{13}C-NMR, ^{29}Si-NMR and FT-IR spectroscopy.

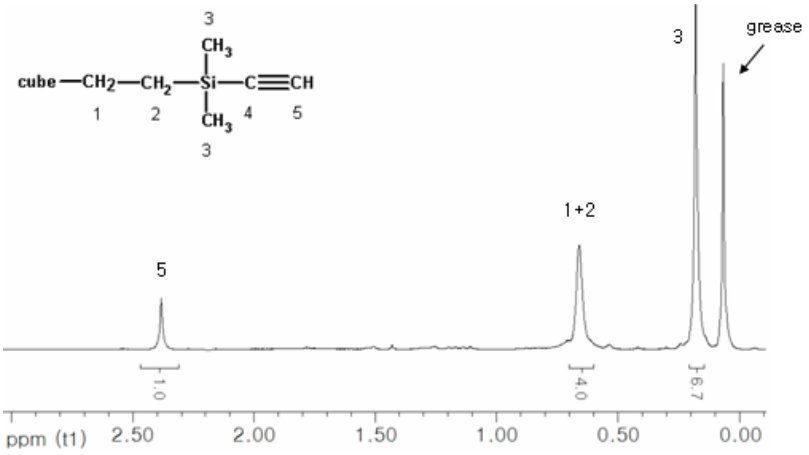

Figure 3.2.4: ^{1}H NMR of POSS^{alkyne}

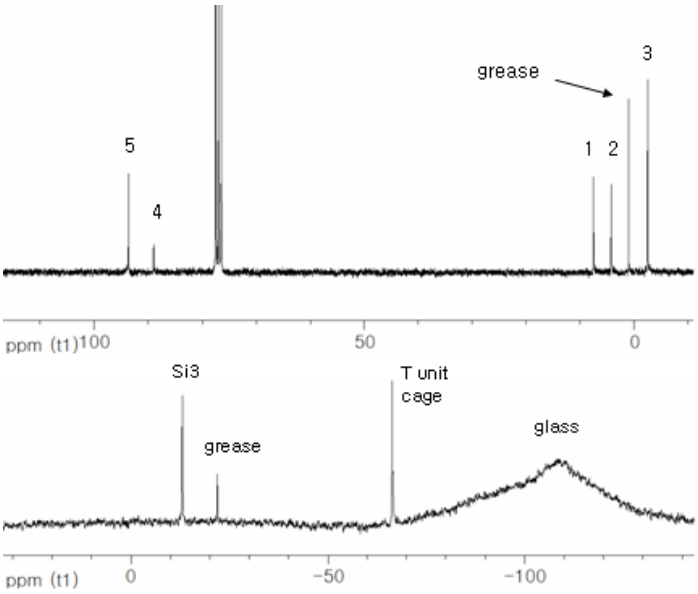

Figure 3.2.5: ^{13}C NMR (up) and ^{29}Si NMR (down) of POSS^{alkyne}

The ^{1}H NMR in Figure 3.2.4 revealed a considerable contamination at 0.067 ppm, which is assigned to grease, which is chemically inert and does not affect the success of the Huisgen 1,3-dipolar cycloaddition reaction. In ^{13}C NMR (Figure 3.2.5) the carbons of the grease can be seen at 1.0 ppm and ^{29}Si NMR (Figure 3.2.5) shows a D unit at -22 ppm, which is as well assigned to grease. The ^{1}H NMR shows the terminal proton of the alkyne at a typical shift of about 2.4 ppm and in the ^{13}C NMR the characteristic shifts of the alkyne carbons are observed at 89 and 93 ppm. The prove that the cage is still intact is given by ^{29}Si NMR with a sharp and single peak at -108.8 ppm, corresponding to the quaternary Si units. As the product has been washed with water, a potential residual chlorine-modified cage would have been hydrolysed and the OH modified cage could be seen in ^{29}Si NMR as an M unit at around 10 ppm.

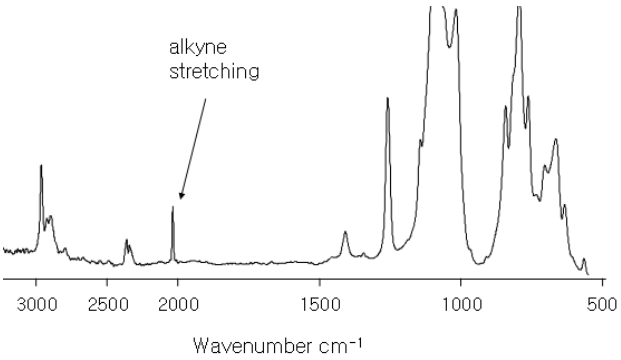

The typical alkyne stretching vibration is observed at 2040 cm^{-1} in the FT-IR spectrum (Figure 3.2.6).

Figure 3.2.6: FT-IR of POSS^{alkyne}

The reaction was selective and quantitative, so that the product did not need any further purification after it had been washed with water to remove the not reacted ethinyl magnesiumbromide.

3.3. Synthesis of Alkyne and Azide modified Polymers

For the introduction of alkyne and azide modified spherosilicates and POSS into polymers by click reaction, polymers with alkyne and azide end-groups are required. Different morphologies can be obtained applying polymers with one or two functional groups.

3.3.1. Synthesis of Alkyne modified Polydimethylsiloxane

As explained in parts 3.1.4 and 3.2.2 a chlorine group next to silicon provides a very good reactivity for the substitution reaction with ethinyl magnesiumbromide. Chlorine end-modified polydimethylsiloxane (PDMS) is commercially available and thus, PDMS is the most easily accessible alkyne modified polymer. On the contrary, azide modified polymers cannot be obtained by reaction of $PDMS^{Cl}$ with sodium azide, because an azide group bonded to a silicon atom is instable[120].

The nucleophilic substitution reaction of $PDMS^{Cl}$ (purchased from Aldrich, M_N=3000) with ethinyl magnesiumbromide was carried out in THF as shown in Scheme 3.3.1. After stirring for 3 hours at room temperature, the solution was washed with saturated NaCl solution to remove excess ethinyl magnesiumbromide.

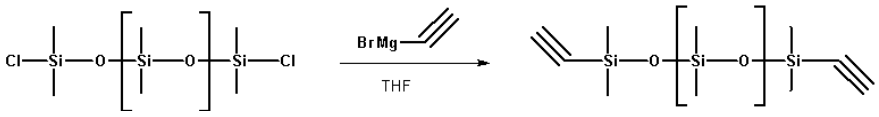

Scheme 3.3.1: Substitution reaction of ethinyl magnesiumbromide with $PDMS^{Cl}$

The product could be obtained with high yields and purity and was characterized by ^{1}H NMR, ^{13}C NMR, ^{29}Si NMR and FT-IR spectroscopy.

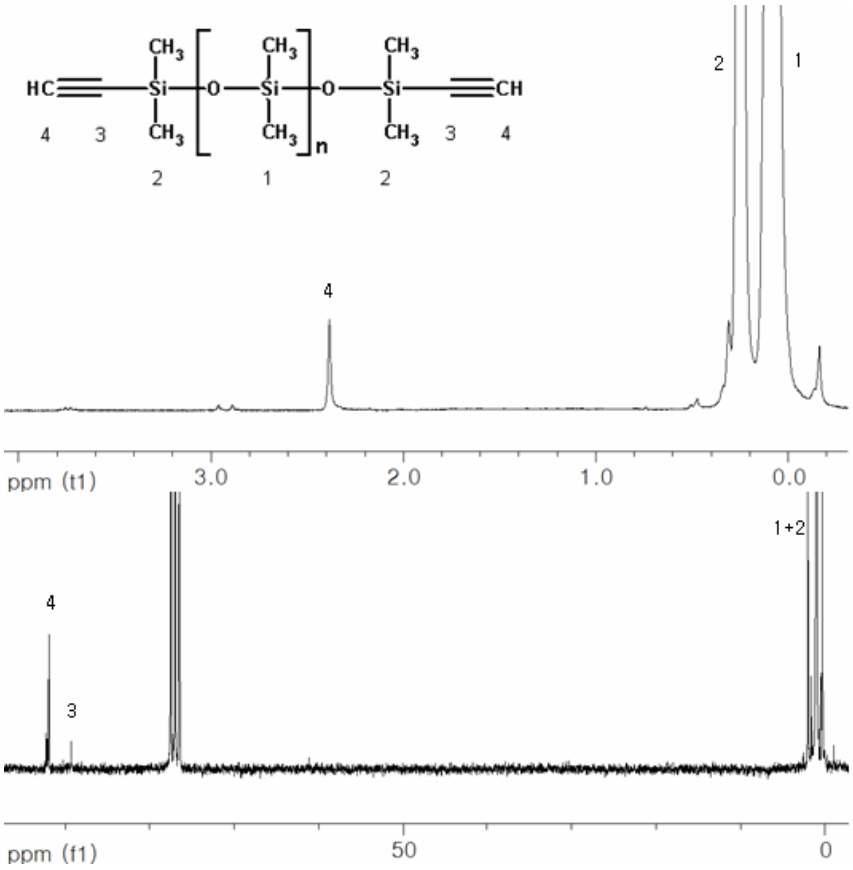

Figure 3.3.1: ^{1}H NMR (up) of PDMS^{alkyne} ^{13}C NMR (down) of PDMS^{alkyne}

In the ^{1}H NMR in Figure 3.3.1 the characteristic shift of the terminal proton of the alkyne is observed at 2.4 ppm and the ^{13}C NMR in Figure 3.3.2 shows the carbons of the alkyne groups at typical shifts of 89 and 92 ppm.

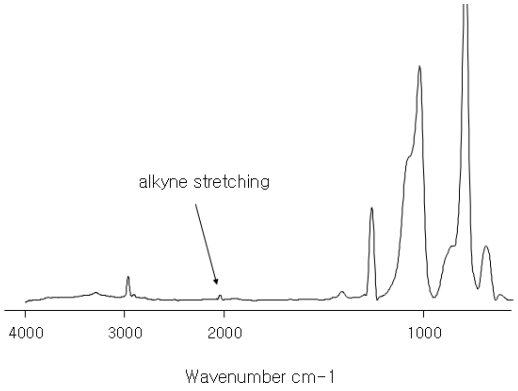

The FT-IR spectrum (Figure 3.3.2) confirms the success of the reaction by the characteristic alkyne stretching vibration at 2040 cm^{-1}.

Figure 3.3.2: FT-IR of PDMS^{alkyne}

Full conversion is proved by ^{29}Si HMBC, where no O-Si$(CH_3)_2$-Cl group (about 10 ppm) can be seen, but 3 different species of silicon. A large peak at -23.8 ppm is assigned to the O-Si$(CH_3)_2$-O groups of the polymer backbone, while the O-Si$(CH_3)_2$ groups next to the

alkyne moiety are shifted to 0.3/-21.5 ppm. A small peak at -21.9/0.1 ppm is assigned to grease.

3.3.2. Synthesis of Azide modified Poly(methyl methacrylate)

Polymers having a functional group that is active for 1,3-dipolar cycloaddition reaction (azide or alkyne) on one chain-end provide the possibility to obtain star-shaped hybrid materials when reacted with eight corner alkyne or azide modified spherosilicates. The most easy and versatile pathway to such polymers is provided by ATRP and subsequent substitution reaction with sodium azide.

According to *Coessens et al.*[74] poly(methyl methacrylate) bearing an azide group on one chain-end can be obtained applying atom transfer radical polymerization (ATRP). This polymerization method provides well defined polymers with halogen end-groups (see introduction) if the polymerization is stopped at low conversions – avoiding recombination and disproportionation reactions by keeping the polymer concentration low.

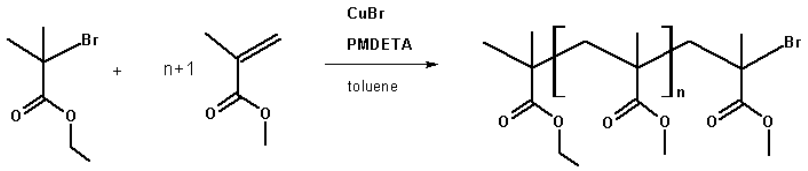

Scheme 3.3.2: ATRP of MMA

The mechanism of this 'quasi-living' polymerization method is explained in the introduction. Polymers with bromine end-groups were prepared using Cu(I)Br and PMDETA as catalyst and ligand and dry toluene as solvent. The molecular weight could be predetermined by the amount of monomer and catalyst, as well as by the reaction time. Polymers with different molecular weights were prepared in order to investigate the effect of the molecular weight on the click reaction with eight corner alkyne modified spherosilicates. The polymers were characterized by ^{1}H NMR, ^{13}C NMR, SEC and FT-IR spectroscopy.

The SEC plot of 3 polymers with different molecular weights in Figure 3.3.4 exhibits polydispersity values around 1.4, which is rather high for a living polymerization method.

This is due to the fact that the polymerization was quenched after short reaction times and low conversion in order to reduce recombination and disproportionation reactions.

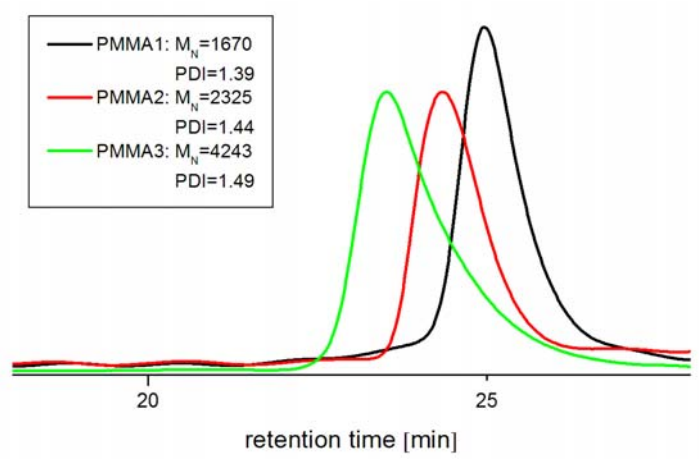

Polymers with defined molecular weights and molecular weight distributions <1.5 having halogen end-groups were prepared using ATRP.

Figure 3.3.4: SEC plot of PMMA with different molecular weights prepared by ATRP

Thus obtained poly(methyl methacrylates) having a bromine group on one chain end can be modified with a variety of functional groups by a S_N2 substitution reaction. Modification with an azide moiety was achieved according to various published works with sodium azide in DMF by stirring for 24 hours at room temperature[74,99,121].

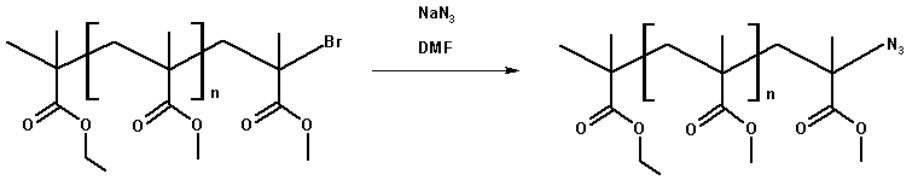

Scheme 3.3.3: Functionalization of PMMA by nucleophilic substitution

The azide end-modified PMMA was characterized by ^{1}H NMR, ^{13}C NMR, SEC and FT-IR spectroscopy. The ^{13}C NMR (Figure 3.3.5) shows the disappearance of the peak at 57 ppm belonging to C-Br and a new peak at 64 ppm, which is assigned to the quaternary carbon next to the azide group.

The FT-IR (Figure 3.3.6) confirms the success of the substitution reaction with the characteristic azide stretching vibration at 2120 cm^{-1}.

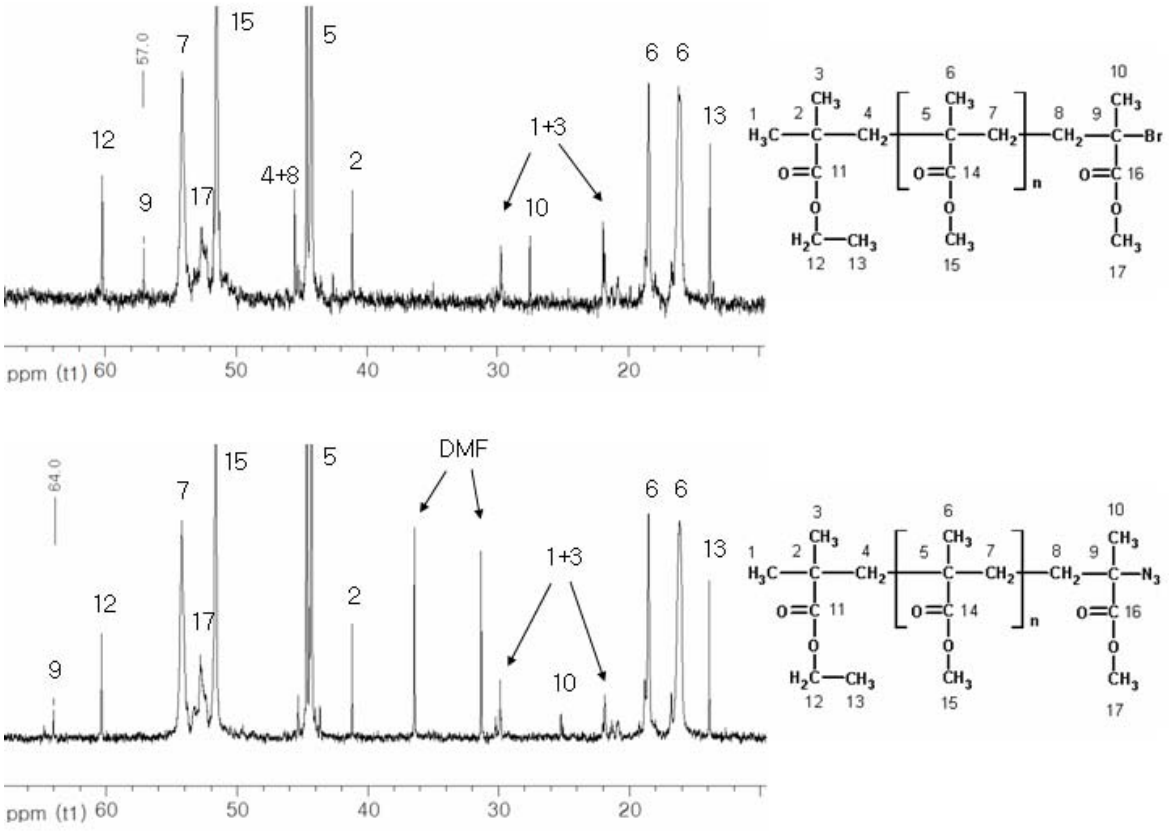

Figure 3.3.5: ^{13}C NMR of PMMA-Br (up) and PMMA-N_3 (down)

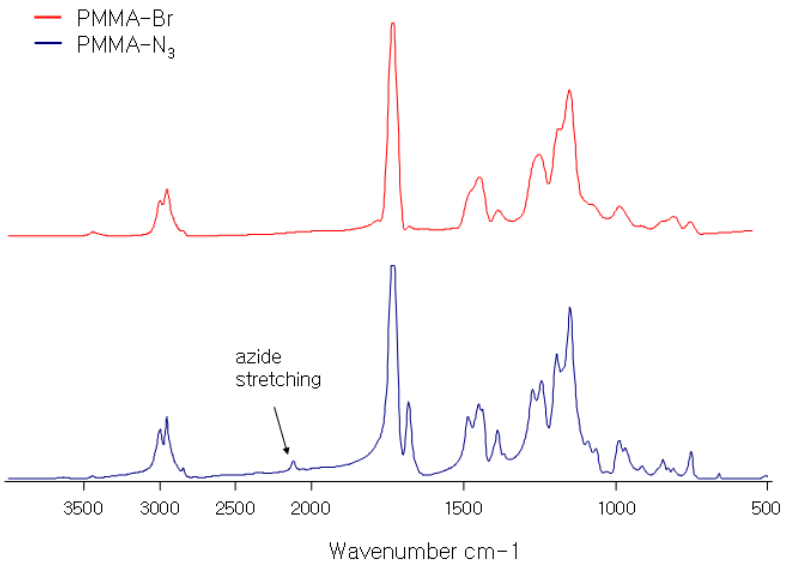

Figure 3.3.6: FT-IR of PMMA-Br (up) and PMMA-N_3 (down)

3.4. Click Reactions

Details about the Huisgen 1,3-dipolar cycloaddition reaction of azides with alkynes were explained in the introduction. According to recent studies, the presence of triazole groups accelerates the click reaction, and for this reason the catalyst system shown in Figure 3.4.1 was applied in all click reactions.

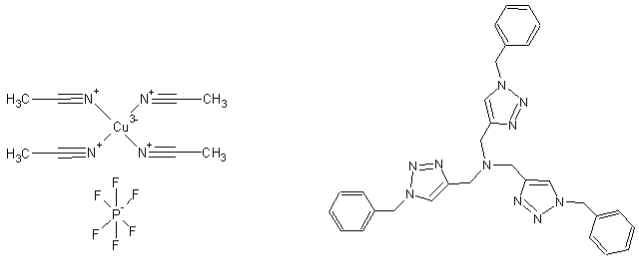

Figure 3.4.1: Cu(I)-Catalyst and Ligand used for the 1,3-dipolar cycloaddition reactions

Having prepared the different building blocks – i.e. $Q_8M_8^{azide}$, $Q_8M_8^{alkyne}$, $POSS^{alkyne}$, $PDMS^{alkyne}$ and $PMMA^{azide}$ – for the Huisgen 1,3-dipolar cycloaddition reaction of azides with alkynes, they can be combined arbitrarily with each other, so that six different click products can be obtained.

Nevertheless the first click reaction to be made was a model reaction with a model azide compound in order to optimize conditions of the click reaction with alkyne modified silica cages without the additional difficulty of the sterical demand of the polymers.

3.4.1. Click Reaction with 1-Azidoadamantane

The click reaction was carried out at room temperature in DMF and water with 1mol% of catalyst (tetrakis(acetonitrile)copper(I)hexafluorophosphate) and ligand (tris(benzyltriazolylmethyl)amine, TBTA) and an access of 1-azidoadamantane according to *Binder et al.*[34].

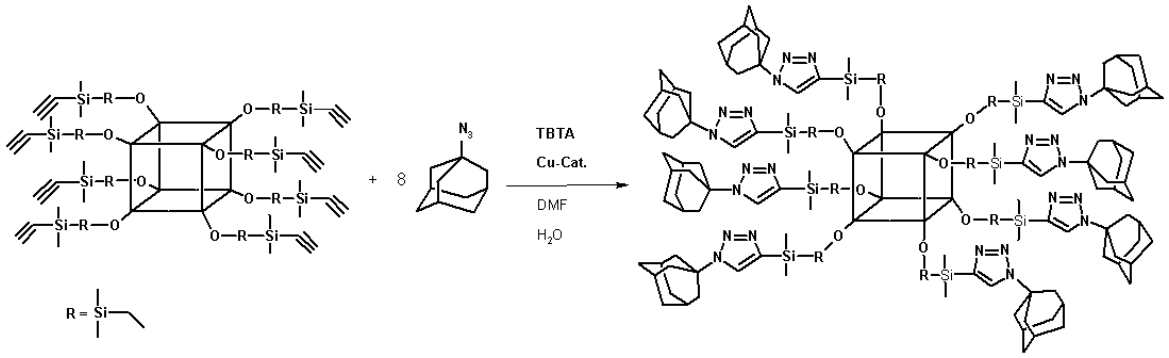

Scheme 3.4.1: Click Reaction of $Q_8M_8^{alkyne}$ with 1-azidoadamantane

After three days of stirring at room temperature, the solvent was evaporated in vacuum at 40°C and the catalyst was removed by column chromatography. The thus obtained product was characterized by ^{1}H NMR, HSQC, HMBC and FT-IR spectroscopy.

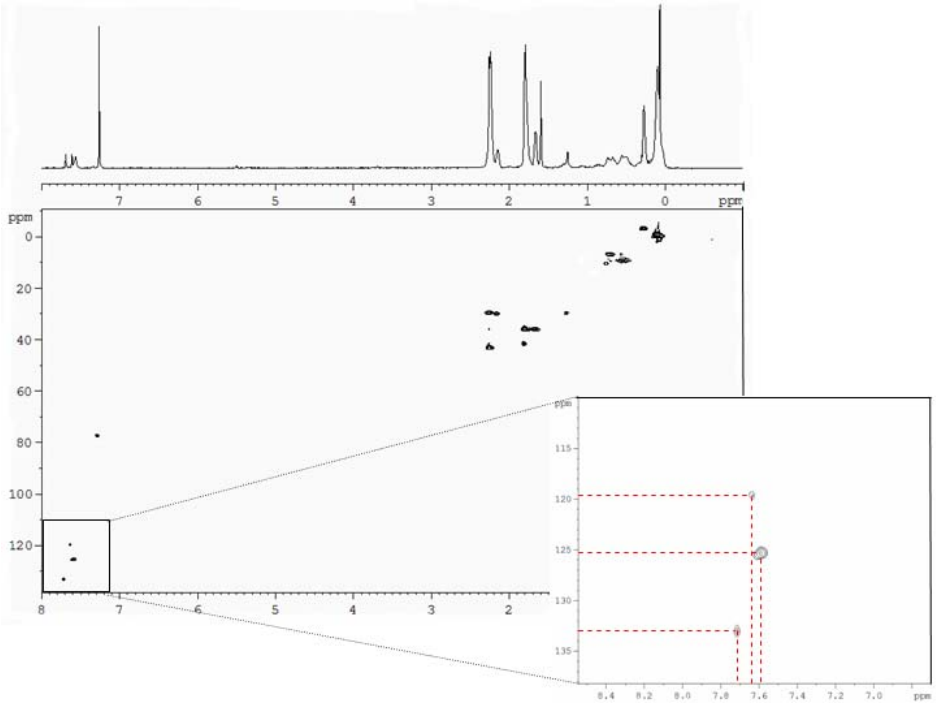

Figure 3.4.2: HSQC spectrum of the click reaction with adamantane azide

The HSQC spectrum (Figure 3.4.2) shows clearly the existence of a triazole by the peaks at ~7.6 ppm, which are coupling with carbons between 120 and 135 ppm, both the protons and the carbons having the characteristic shifts of triazole C-H.

The adamantane-protons are observed at their typical shifts around 2 ppm correlating with carbons between 20 and 40 ppm, while the protons of the alkyl chain connecting the

spherosilicate with the adamantane are obvious between 0 and 1 ppm correlating with carbons between -2 and 10 ppm.

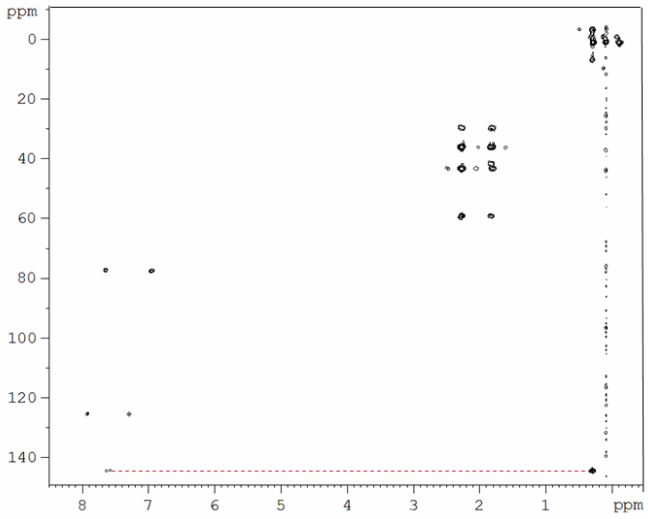

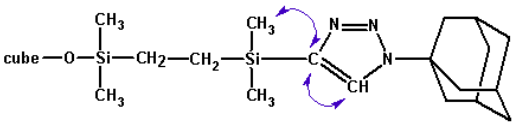

The HMBC spectrum shows that the CH_3 group belonging to the spherosilicate is coupling with the quaternary carbon of the triazole, which is characteristically shifted to 145 ppm.

Figure 3.2.3: HMBC spectrum of the click reaction with 1-azidoadamantane

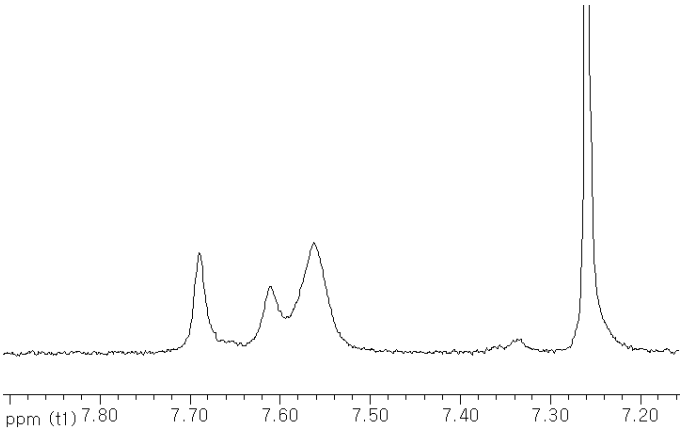

In the ^1H NMR (Figure 3.4.4), two different species of triazoles can be seen, which might be due to different interactions between differently functionalized corners.

Figure 3.4.4: ^1H NMR of the click reaction with adamantane azide

According to *Rostovtsev et al.*[87], the formation of 1,5-adducts should be avoided by using the copper catalyzed version of the Huisgen 1,3-dipolar cycloaddition. Thus it is supposed that the three different shifts are due to not full eight corner functionalization, which leads to different interactions between functionalized and non-functionalized corners.

Hence the success of the click reaction is proved, the only drawback being that not all eight corners could be functionalized.

3.4.2. Click Reactions with Polymers

Due to lack of time, click reactions with polymers could not be carried out yet. Future studies will include optimizations on the click reaction with adamantane azide using other catalyst systems and solvents, as well as click reactions between spherosilicates of POSS and polymers in order to obtain hybrid materials. Moreover, we are optimistic that click reactions between azide and alkyne modified silica cages will result in highly porous materials.

4. Conclusions

Aim of this thesis was the synthesis of modified spherosilicates and polyhedral oligomeric silsesquioxanes as building blocks for the Huisgen 1,3-dipolar cycloaddition reaction of azides with alkynes and the click chemistry bond formation with polymers.

The motivation of this approach was the possibility to obtain nanocomposites by a simple reaction that can be carried out using simple reaction conditions and does not give any unwanted by-products. Moreover the building block system provides the possibility of combining the modified spherosilicates arbitrarily with any azide or alkyne functionalized compound.

4.1. Summary of the Functionalization Reactions of Spherosilicates

Four possible pathways for the synthesis of alkyne and azide modified spherosilicates were studied, all of them based on the functionalization of a spherosilicate octaanion by reaction with chlorosilanes.

In the first approach the literature known functionalization with chloro(chloromethyl)dimethylsilane was studied and optimized. The obtained chlorine-functionalized spherosilicate was allowed to react with sodium acetylide and ethinyl magnesiumbromide in order to obtain alkyne modified cages. The reaction with sodium acetylide was partly successful, but we were not able to yield full eight corner functionalization. Substitution reaction of the chlorine functionalized spherosilicate with ethinyl magnesiumbromide was not successful.

Modification of the spherosilicate with azide groups was partly successful reacting the chlorine modified cage with sodium azide. Unfortunately, even applying elevated temperatures and long reaction times it was not possible to obtain eight corner functionalization. On the contrary, when kept at elevated temperatures for more than 3 days, the azide groups decomposed.

These results suggested that for the synthesis of spherosilicates having azide or alkyne groups on all eight corners a more reactive leaving group had to be provided. It is well known, that bromine is a better leaving group for S_N2 substitution reactions, than chlorine. For this reason, allyl bromide was hydrosilated with a spherosilicate having Si-H groups on all eight corners in a literature known reaction. It was found that this reaction does not

provide the desired product, but side reactions that occurred in a similar way as in the case of allyl chloride lead to a crosslinked spherosilicate.

A tosylate-modified cage was targeted in a further approach, which would also provide a good leaving group for nucleophilic substitution reactions. Thus, $Q_8M_8^H$ was modified with a hydroxy group by hydrosilation reaction with allyl alcohol applying a literature known reaction. Although a literature procedure described that O-silylation as a side reaction can be suppressed by using high concentrations of Karstedt's catalyst and allyl alcohol, a partly crosslinked product was obtained most likely due to a small amount of C- and O-silylated chains as determined by SEC. However, a small amount of crosslinked cages does not influence the properties of a potential hybrid material. Thus, the obtained eight corner hydroxy modified spherosilicate was used for the preparation of tosylate modified cages. The reaction was successful and the eight corner tosylate modified spherosilicate could be obtained in high yields and also the amount of crosslinked cages could be reduced by column chromatography.

Reaction of the tosylate modified spherosilicate with sodium azide provided an eight corner azide modified spherosilicate and thus the first building block for the click reactions.

Various attempts to convert the tosylate into alkyne groups by reaction with sodium acetylide and ethinyl magnesiumbromide failed. Thus, in a fourth approach spherosilicates having highly reactive silicon-chlorine bonds were prepared by a literature known reaction. The chlorine groups were successfully substituted with alkyne groups by reaction with ethinyl magnesiumbromide and thus a second building block for the Huisgen 1,3-dipolar cycloaddition reaction of azides with alkynes was provided.

4.2. Summary of the Functionalization Reactions of POSS

Two synthetic methods to alkyne modified POSS were studied, the first one being the direct hydrolysis/condensation of ethinyltriethoxysilane. This method did not lead to the desired product. It is assumed that TBAF coordinates to alkynes releasing HF, so that the required F^- is not available for the controlled hydrolysis/condensation reaction.

The second synthesis from commercially obtained chlorine modified POSS provides a simple and efficient way to eight corner alkyne modified spherosilicates, the reaction

results in full conversion and high yields and does not require any time-consuming purification steps.

4.3. Summary of the Functionalization Reactions of Polymers

For the preparation of modified polymers two different systems were chosen according to the accessibility of polymer chains bearing functional groups on one or on both chain ends. Thus, different morphologies (star polymers and crosslinked networks) can be obtained by click reactions with silica cages.

Polydimethylsiloxane having chlorine groups on both chain ends is commercially available and thus, PDMS is the most easily accessible polymer with two functional groups. A chlorine group next to silicon provided a very good reactivity for the substitution reaction with ethinyl magnesiumbromide. The reaction was successful with full conversion and provided a fourth building block for the click reaction.

On the contrary, azide modified polymers cannot be obtained by reaction of $PDMS^{Cl}$ with sodium azide, because an azide group bonded to a silicon atom is instable[120].

ATRP is a very versatile tool towards polymers with defined molecular weights having a halogen end-group on one chain end. For this reason, poly(methyl methacrylate) was prepared by ATRP, followed by substitution reaction with sodium azide. PMMA with an azide group on one chain end was prepared applying this route, providing the fifth building block for the click reaction.

4.4. Summary of the Click Reaction

Having prepared the different building blocks – i.e. $Q_8M_8^{azide}$, $Q_8M_8^{alkyne}$, $POSS^{alkyne}$, $PDMS^{alkyne}$ and $PMMA^{azide}$ – for the Huisgen 1,3-dipolar cycloaddition reaction of azides with alkynes, they can be combined arbitrarily with each other, so that six different click products could be obtained. Nevertheless, the first click reaction to be made was a model reaction with a ‘small’ azide in order to optimize the click reaction with alkyne modified silica cages without the additional difficulty of the sterical demand of the polymers.

The model click reaction was successful, even if not all eight corners could be functionalized with adamantane.

5. Experimental Part

Measurements

NMR spectra were recorded on a 300-MHz DRX Avance Bruker instrument working at 300, 75.43 and 59.6 MHz for ^{1}H, ^{13}C and ^{29}Si, respectively. Relative size exclusion chromatography (SEC) were performed with a Waters system, which included a 515 HPLC pump, a 717 autosampler, a 2410 differential refractive index detector and Styragel columns (HR 0.5, 3, 4, linear), at 40°C at a rate of 1 ml/min. The system was calibrated using linear polystyrene standards. The molecular weight analysis was calculated with Waters Millennium software that included the GPC/V option, and it was related to an internal standard (diphenyl ether). Fourier transform infrared spectra were recorded on a Bruker Tensor27 spectrometer using ATR technique. Elemental analysis was carried out in the microanalytic laboratory of the institute of physical chemistry at the University of Vienna.

Materials

Toluene (99%, Merck), n-hexane (95%, Acros), dichloromethane (98%, Riedel-de Haen), dimethylformamide (DMF, Aldrich) and dimethyl sulfoxide (DMSO, 99+%, Aldrich) were dried and distilled from CaH_2 and stored under an argon atmosphere. Tetrahydrofurane (THF, 99%, Fluka) was dried and distilled from benzophenone-Na. Methyl methacrylate (MMA, 99%, Aldrich) was distilled from CaH_2 and stored under an argon atmosphere at -15°C. Allyl alcohol (98.5+%, Aldrich) and allyl bromide (99%, Aldrich) were freshly distilled before use. Copper(I)-bromide (CuBr, 98+%, Fluka) was purified by stirring in acetic acid overnight, washing with dry n-hexane and drying. Ethyl-2-bromoisobutyrate (EiBr, 98% Aldrich) and N,N,N',N'',N''-pentamethyldiethylenetriamine (PMDETA, 99%, Aldrich) were distilled before use. Platinum(0)-1,3-divinyl-1,1,3,3-tetramethyl-disiloxane complex (Pt(dvs), Karstedt's-catalyst) was obtained from Aldrich (0.1 M solution in poly(dimethylsiloxane), vinyl terminated) and diluted to a 2 mM solution in distilled toluene before use. All other

chemicals – except tetraethoxysilane (TEOS, 98+%, Fluka), chlorodimethylvinylsilane (Wacker) and tetrabutylammoniumfluoride (TBAF, Acros Organics) – were purchased by Aldrich and used as received.

Experiments

All experiments were carried out under an argon atmosphere using schlenk technique.

5.1. Preparation of modified spherosilicates

5.1.1. Preparation of octakis(tetramethylammonium)octasilsesquioxane ($Q_8M_8^-$) (1):

This compound was obtained following a procedure by *Holzinger* and *Kickelbick*[10]. 67.5 g (0.170 mol) of 25% tetramethylammonium hydroxide was provided in a 500 ml round bottom flask equipped with a magnetic stirrer. 27.69 g (0.864 mol) of methanol and 25.0 g (1.389 mol) of water were added and after 10 min of stirring, 35.417 g (0,170 mol) of tetraethoxysilane was added via a syringe. The reaction mixture was stirred for 48 hours at room temperature. The white precipitate was separated and rejected and the resulting solution was used without any further characterization.

5.1.2. Preparation of octakis[(chloromethyl)dimethylsiloxy]octasilsesquioxane ($Q_8M_8^{CH_2Cl}$) (2):

The synthesis differs from the literature procedure[45]. In a 250 ml round bottom flask equipped with an argon inlet, a dropping funnel and a magnetic stirrer, 6.82 g (47.7 mmol) chloromethyldimethylchlorosilane was dissolved in 30 mL heptane. To this mixture 12 mL (1.49 mmol) of the octaanion solution (1) was added dropwise. After 15 minutes of stirring at 4°C and 30 minutes of stirring at room temperature, the heptane phase was

separated. The water phase was extracted 3 times with heptane. The collected organic phases were dried over $MgSO_4$ and the solvent was evaporated from the filtered solution. The product was purified by recrystallization from acetonitrile.

Yield: 0.69 g (33%)

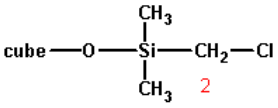

^{1}H NMR (δ, $CDCl_3$): 2.75 [s, 2H, 2], 0.21 [s, 6H, 1].
^{13}C NMR (δ, $CDCl_3$): 29.9 [2], -1.9 [1].
^{29}Si NMR (δ, $CDCl_3$): -109.4 [cube], 8.4 [Si 1].

FT-IR (cm^{-1}): υ CH_3: 2963; υ Si-CH_3: 1395, 1257, 846; υ Si-C: 1180; υ Si-O: 1071; υ C-Cl: 823, 800.

Elemental analysis: calculated: C: 20.51%, H: 4.59%, Cl: 20.18%. Found: C: 20.81%, H: 4.31%, Cl: 19.72%.

5.1.3. Reaction of $Q_8M_8^{CH_2Cl}$ (2) with sodium acetylide:

In a 50 ml round bottom flask equipped with an argon inlet and a magnetic stirrer 1.2 g (4.5 mmol) of sodium acetylide (18% slurry in xylene and mineral oil) were dissolved in 7.5 ml of dry DMF and 12.5 ml of dry toluene under an argon atmosphere. The fully chlorine functionalized spherosilicate (2) was dissolved in dry toluene and added to the prepared sodium acetylide solution. After stirring for 24 hours at room temperature the reaction was quenched with saturated NH_4Cl solution. The organic phase was dried over $MgSO_4$ and the solvent was removed under reduced pressure. The product was obtained as a brown oil.

^{1}H NMR (δ, $CDCl_3$): 2.75 [s, 2H, CH_2Cl], 2.07 [s, $\underline{CH_2}$-C≡CH], 1.91 [C≡$\underline{CH}$], 0.21 [s, 6H, Si($\underline{CH_3}$)$_2$-CH_2-Cl], 0.03 [Si($\underline{CH_3}$)$_2$-CH_2-C≡CH]
^{13}C NMR (δ, $CDCl_3$): 80.4 [C≡CH], 72.3 [C≡CH], 29.9 [CH_2Cl], 5.3 [CH_2-C≡CH], 1.3 [Si(CH_3)$_2$-CH_2-C≡CH], -1.9 [Si(CH_3)$_2$-CH_2-Cl].

5.1.4. Reaction of $Q_8M_8^{CH_2Cl}$ (2) with ethinyl magnesiumbromide:

In a 100 ml round bottom flask equipped with a magnetic stirrer and an argon inlet 0.3 g (0.2 mmol) of the fully chlorine modified spherosilicate (2) was dissolved in 20 ml of dry THF under an argon atmosphere. Ethinyl magnesiumbromide (6.4 ml 0.5 M solution in THF, 3.2 mmol) was added via a syringe. The reaction mixture was stirred for 48 hours at 40 °C, then diluted with diethyl ether and washed with saturated NaCl. The aqueous layer was washed two times with diethyl ether and the combined organic layers were dried over $MgSO_4$. The solvent was evaporated from the filtered solution.

^{1}H NMR (δ, $CDCl_3$): 2.75 [s, 2H, CH_2-Cl], 0.21 [s, 6H, $Si(CH_3)_2$].
^{13}C NMR (δ, $CDCl_3$): 29.9 [CH_2-Cl], -1.9 [$Si(CH_3)_2$].

5.1.5. Reaction of $Q_8M_8^{CH_2Cl}$ (2) with sodium azide:

In a 50 ml round bottom flask equipped with an argon inlet and a magnetic stirrer 0.07 g (1.0 mmol) of sodium azide was dissolved in a mixture of dry THF and dry DMF (4:5) under an argon atmosphere. 0.1 g (0.07 mmol) of the fully chlorine substituted spherosilicate was dissolved in dry DMF and added to the prepared sodium azide solution via a syringe. After stirring for 24 hours at room temperature the reaction mixture was washed with water. The water phase was extracted with diethyl ether and the organic phase was dried over $MgSO_4$. The solvent was evaporated under reduced pressure and the product was obtained as a white solid.

^{1}H NMR (δ, $CDCl_3$): 2.75 [s, CH_2Cl], 0.21 [s, $Si(CH_3)_2$]
^{13}C NMR (δ, $CDCl_3$): 29.9 [CH_2Cl], -1.9 [$Si(CH_3)_2$]

5.1.6. Preparation of octakis(dimethylsiloxy)octasilsesquioxane cube ($Q_8M_8^H$) (3):

This compound was obtained following a procedure by *Holzinger* and *Kickelbick*[10]. In a 500 ml round bottom flask with an argon inlet, a dropping funnel and a magnetic stirrer 10.65 g (0.11 mol) of chlorodimethylsilane in 150 ml of n-hexane was cooled to 0°C under an argon atmosphere. To this mixture, 85 ml (0.012 mol) of the octaanion solution (1) was added slowly. After 1 hour of stirring at 4°C and 4 hours of stirring at room temperature, the hexane phase was separated. The water phase was extracted 3 times with hexane. The collected organic phases were dried over $MgSO_4$ and the solvent was evaporated from the filtered solution.

Yield: 7.24 g (59%) of a white solid.

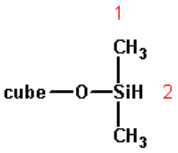

^{1}H NMR (δ, $CDCl_3$): 4.7 [t, J=2.57Hz, 8H, 2], 0.3 [d, J=2.57Hz, 48H, 1].
^{13}C NMR (δ, $CDCl_3$): 0.05 [1].
^{29}Si NMR (δ, $CDCl_3$): 0.2 [$(CH_3)_2$SiH], -108.0 [Si-O-Si, cube].

FT-IR (cm^{-1}): υ CH_3: 2963; υ Si-H: 2140; υ Si-CH_3: 1422, 1255, 835, 762; υ Si-O: 1058.

5.1.7. Hydrosilation of allyl bromide with octakis(dimethylsiloxy)octasilsesquioxane cube ($Q_8M_8^H$) with Speier's catalyst:

This reaction was performed according to the following procedure by *Provatas et al.*[111]. In a 50 ml round bottom flask equipped with an argon inlet, a reflux condenser and a magnetic stirrer 0.2 g (0.2 mmol) of $Q_8M_8^H$ (3) was dissolved in 5 ml of dry diethyl ether under an argon atmosphere, followed by addition of H_2PtCl_6 (1 drop of 1% solution in dry DMF). 0.24 g (2.0 mmol) of allyl bromide was added via syringe and the reaction mixture was stirred for 24 hours at room temperature and then heated to reflux for 3 days. The white precipitate was separated and the solvent was evaporated from the solution under reduced pressure.

Characterization data of the soluble compound: ^{1}H NMR (δ, $CDCl_3$): 4.73 [residual Si-H], 0.25 [O-Si($\underline{CH_3}$)$_2$-O], 0.3 [residual Si($\underline{CH_3}$)$_2$-H]. ^{13}C NMR (δ, $CDCl_3$): 1.1 [Si(CH_3)$_2$]. ^{29}Si NMR (δ, $CDCl_3$): 0.2 [(CH_3)$_2$$\underline{Si}$H], -8.9, -20.0, -22.9 [Si-Br, Si-OH, Si-O-Si].

Characterization data of the insoluble compound: FT-IR (cm^{-1}): υ CH: 2961, 2911; 2702, 2476, Si-H: 2127, 1668, 1475, Si-CH_3: 1411, 1262, 852, 806; Si-C: 1140: Si-O: 1096, 1052.

5.1.3. Hydrosilation of allyl bromide with octakis(dimethylsiloxy)octasilsesquioxane cube ($Q_8M_8^H$) with Karstedt's catalyst:

This reaction was performed according to the following procedure by *Zhang* and *Laine*[113] for the Hydrosilation of allyl alcohol[113]. In a 25 ml round bottom flask equipped with an argon inlet, a reflux condenser and a magnetic stirrer 0.2 g (0.2 mmol) of $Q_8M_8^H$ (3) was dissolved in 5 ml of dry diethyl ether under an argon atmosphere, followed by addition of 0.24 g (2.0 mmol) of allyl bromide. The reaction flask was evacuated and refilled with argon three times. Pt(dvs) (2mM solution, 0.5 ml) was added via a syringe and the reaction mixture was stirred for 24 hours at room temperature and then heated to reflux for 3 days. The white precipitate was separated and the solvent was evaporated from the solution under reduced pressure.

Characterization data of the soluble compound: ^{1}H NMR (δ, $CDCl_3$): 4.73 [residual Si-H], 0.25 [O-Si($\underline{CH_3}$)$_2$-O], 0.3 [residual Si($\underline{CH_3}$)$_2$-H]. ^{13}C NMR (δ, $CDCl_3$): 1.1 [Si(CH_3)$_2$]. ^{29}Si NMR (δ, $CDCl_3$): 0.2 [(CH_3)$_2$$\underline{Si}$H], -8.9, -20.0, -22.9 [Si-Br, Si-OH, Si-O-Si].

Characterization data of the insoluble compound: FT-IR (cm^{-1}): υ CH: 2961, 2911; 2702, 2476, Si-H: 2127, 1668, 1475, Si-CH_3: 1411, 1262, 852, 806; Si-C: 1140: Si-O: 1096, 1052.

5.1.4. Preparation of octakis[(3-hydroxypropyl)dimethylsiloxy]octasilsesquioxane ($Q_8M_8^{OH}$) (4) by direct hydrosilation reaction:

This compound was obtained following a procedure by *Zhang* and *Laine*[113]. In a 100 ml round bottom flask equipped with an argon inlet and a magnetic stirrer 6.00 g of (5.9 mmol) $Q_8M_8^H$ (2) was dissolved in 30 ml of dry toluene under an argon atmosphere, followed by addition of 5.58 g (94.4 mmol) of allyl alcohol. The reaction flask was evacuated and refilled with argon three times. Pt(dvs) (2mM solution, 2.0 ml) was added via a syringe. The reaction mixture began to reflux immediately. After 1 hour the solution had cooled to room temperature and two layers were formed. PPh_3 (~20 mg), was added and the mixture was stirred for ~1 hour. The bottom layer containing the product, was recovered. Residual allyl alcohol and toluene were removed first under argon stream, and then under vacuum.

Yield: 7.9 g (90%) of a white solid.

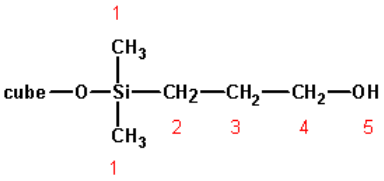

^{1}H NMR (δ, CD_3OD): 3.52 [bs, 16H, 4], 1.59 [bs, 16H, 3], 0.65 [bs, 16H, 2], 0.19 [s, 48H, 1].

^{13}C NMR (δ, CD_3OD): 65.1 [4], 26.0 [3], 13.3 [2], -0.39 [1].

FT-IR (cm^{-1}): υ OH: 3334 broad, 1412; υ CH_3: 2930, 2873; υ Si-CH_3: 1254, 1166, 833, 781; υ Si-O: 1053.

5.1.7. Preparation of octakis[dimethyl(3-toluenesulfonylpropyl)siloxy]octasil sesquioxane ($Q_8M_8^{OTos}$) (5):

In a 250 ml round bottom flask equipped with an argon inlet and a magnetic stirrer 7.9 g (5.33 mmol) of $Q_8M_8^{OH}$ (4) was dissolved in 120 ml of dry dichloromethane under an argon atmosphere. 16.18 g (0.16 mol) of triethylamine, 0.39 g (3.20 mmol) of 4-(dimethylamino)pyridine (DMAP) and 12.19 g (63.9 mmol) of p-toluenesulfonyl chloride were added in this order. The reaction mixture was stirred for 24 hours at room temperature, then transferred to a 500 ml extraction funnel, diluted with n-hexane (250 ml)

and washed with water (15 ml). The aqueous layer was extracted with dichloro methane (3 x 20 ml). The combined organic layers were washed with saturated $NaHCO_3$ (30 ml) and saturated NaCl (30 ml) and dried over $MgSO_4$. The solvent was evaporated from the filtered solution. Purification by column chromatography (50:1 chloroform/methanol) afforded the pure product.

Yield: 7.92 g (54%) of a brown oil.

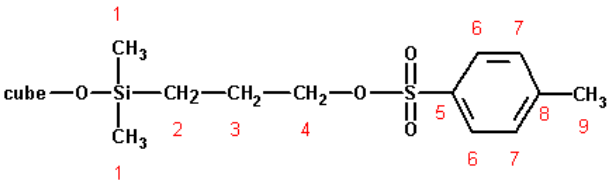

^{1}H NMR (δ, $CDCl_3$): 7.76 [d, J=7.7Hz, 2H, 6], 7.33 [d, J=7.8Hz, 2H, 7] , 3.94 [s, 16H, 4], 2.43 [s, 24H, 9], 1.63 [s, 16H, 3], 0.52 [s, 16H, 2], 0.07 [s, 48H, 1].

^{13}C NMR (δ, $CDCl_3$): 144.6 [8], 133.1 [5], 129.8 [7], 127.8 [6], 72.6 [4], 22.6 [9], 21.6 [3], 13.0 [2], -0.46 [1].

^{29}Si NMR (δ, $CDCl_3$): 12.5 [Si 1], -107.47, -108.43 [cage, cage with O-silylated corners]

FT-IR (cm^{-1}): υ CH_3: 2959; υ ring: 1597; υ SO_2: 1356; υ Si-CH_3: 1258, 1174, 805; υ Si-O: 1063; υ tosylate: 956, 898.

5.1.8. Preparation of octakis[(3-azidopropyl)dimethylsiloxy]octasilsesquioxane ($Q_8M_8^{azide}$) (6):

In a 25 ml round bottom flask equipped with an argon inlet and a magnetic stirrer 0.1 g (0.037 mmol) of $Q_8M_8^{OTos}$ (5) was dissolved in 5 ml of dry DMF under an argon atmosphere. 0.15 g (2.34 mmol) of NaN_3 was added and the reaction mixture was stirred for 24 hours at room temperature. The solution was diluted with ethyl acetate and washed with saturated NH_4Cl and saturated NaCl. The organic layer was dried over $MgSO_4$ and the solvent was evaporated from the filtered solution and the product was obtained as a brown oil.

Yield: 0.04 g (67%)

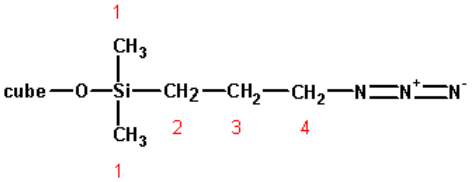

^{1}H NMR (δ, $CDCl_3$): 3.25 [t, J=6.5Hz, 16H, 4], 1.65 [bs, 16H, 3], 0.65 [bs, 16H, 2], 0.17 [s, 48H, 1].

^{13}C NMR (δ, $CDCl_3$): 54.16 [4], 22.76 [3], 14.73 [2], -0.38 [1].
^{29}Si NMR (δ, $CDCl_3$): 12.4 [Si 1], -107.0 + -108.3 [cage, cage with O-silylated corners]

FT-IR (cm^{-1}): υ CH_3: 2959; υ N_3: 2095; υ Si-CH_3: 1450, 1254, 837, 803; υ Si-C: 1169; υ Si-O: 1060.

5.1.9. Reaction of $Q_8M_8O^{Tos}$ with sodium acetylide:

A suspension of sodium acetylide (0.94 g of an 18 wt % suspension in mineral oil) was filtered and washed with dry n-hexane under an argon atmosphere to remove mineral oil (5 x 5 ml). Traces of hexane were removed under reduced pressure to provide sodium acetylide powder (0.17 g, 3.51 mmol). The powder was dissolved in dry DMSO and added to a solution of $Q_8M_8^{OTos}$ (5) (0.30 g, 0.11 mmol) in dry DMSO in a 50 ml round bottom flask equipped with an argon inlet and a magnetic stirrer at 15°C. After 2 hours of stirring at room temperature the deep red reaction mixture was quenched with saturated NH_4Cl (7 ml) and solid NH_4Cl (~ 0.1 g) and the aqueous phase was extracted with ether. The combined organic phases were dried over Na_2SO_4 and the solvent was evaporated from the filtered solution.

^{1}H NMR (δ, $CDCl_3$): 3.52 [t, J=6.67Hz, 16H, $\underline{CH_2}$-OH], 1.71 [bs, 1H, OH]1.59 [p, J=6.71Hz, 16H, $\underline{CH_2}$-CH_2-OH], 0.65 [m, J= 16H, $Si(CH_3)_2$-$\underline{CH_2}$], 0.19 [s, 48H, $Si(CH_3)_2$].
^{13}C NMR (δ, $CDCl_3$): 65.1 [$\underline{CH_2}$-OH], 26.0 [$\underline{CH_2}$-CH_2-OH], 13.3 [$Si(CH_3)_2$-$\underline{CH_2}$], -0.39 [$Si(CH_3)_2$].

5.1.10. Reaction of $Q_8M_8^{OTos}$ with ethinyl magnesiumbromide:

In a 50 ml round bottom flask equipped with an argon inlet, a reflux condenser and a magnetic stirrer 0.7 g (0.26 mmol) of $Q_8M_8^{OTos}$ (5) was dissolved in 10 ml of dry THF under an argon atmosphere. Ethinyl magnesiumbromide (7.0 ml 0.5 M solution in THF, 2.56 mmol) was added via syringe. The reaction mixture was stirred for 48 hours at 40 °C, then diluted with diethyl ether and washed with saturated NaCl. The aqueous layer was

washed two times with diethyl ether and the combined organic layers were dried over $MgSO_4$. The solvent was evaporated from the filtered solution.

^1H NMR (δ, $CDCl_3$): 3.39 [t, J=6.84Hz, 2H, CH_2-Cl/Br], 1.89 [bs, 2H, CH_2-CH_2-CH_2], 0.72 [bs, 2H, $Si(CH_3)_2$-CH_2], 0.17 [s, 6H, $Si(CH_3)_2$]. ^{13}C NMR (δ, $CDCl_3$): 36.8 [CH_2-Cl/Br], 27.1 [CH_2-CH_2-CH_2], 16.5 [$Si(CH_3)_2$-CH_2], -0.1 [$Si(CH_3)_2$].

FT-IR (cm^{-1}): υ CH_3: 2958; υ CH_2: 2927; υ ring (residual tosylate): 1599, 1156, 791; υ Cl-CH_2: 1434; υ SO_2 (residual tosylate): 1362; υ Si-CH_3: 1410, 1255, 838; υ Si-C: 1176; υ Si-O: 1064.

5.1.11. Preparation of octakis(dimethylvinylsiloxy)octasilsesquioxane cube ($Q_8M_8^{vinyl}$) (7):

This compound was obtained following a procedure by *Hasegawa* and *Motojima*[122]. In a 500 ml round bottom flask equipped with an argon inlet and a magnetic stirrer 26.96 g (0.28 mol) of chlorodimethylvinylsilane in 150 ml of THF was cooled to 0°C under an argon atmosphere. 85 ml (0.012 mol) of the octaanion solution (1) was added slowly to this mixture. After 1 hour of stirring at 0°C and 4 hours of stirring at room temperature, the solution was diluted with water and n-hexane. The hexane phase was separated and washed 3 times with water. The organic phase was dried over $MgSO_4$ and the solvent was evaporated from the filtered solution. After washing with methanol to remove the not fully eight corner functionalized cages the pure product was obtained as a white powder.

Yield: 8.32 g (56%)

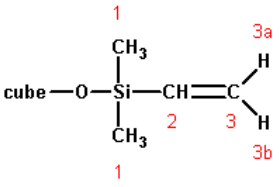

^1H NMR (δ, $CDCl_3$): 6.13 [dd, J_1=19.69Hz, J_2=14.88Hz, 8H, 3a], 5.96 [dd, J_1=14.88Hz, J_2=4.46Hz, 8H, 3b], 5.78 [dd, J_1=19.69Hz, J_2=4.46Hz, 8H, 2], 0.21 [s, 48H, 1].
^{13}C NMR (δ, $CDCl_3$): 137.9 [3], 132.5 [2], -0.23 [1].

FT-IR (cm^{-1}): υ =C-H: 3058; υ CH_3: 2965, 2904; υ C=C: 1601, 1413; υ Si-CH_3: 1262, 840, 788; υ Si-C: 1170; υ Si-O: 1093; υ Si-CH=CH_2: 1009, 958.

5.1.12. Preparation of octakis[(2-chlorodimethylsilylethyl)dimethylsiloxy] octasilsesquioxane ($Q_8M_8^{Cl}$) (8):

The synthesis differs slightly from the literature procedure[116]. In a 100 ml round bottom flask equipped with an argon inlet and a magnetic stirrer 4.00 g (3.30 mmol) of $Q_8M_8^{vinyl}$ (7) was dissolved in 40 ml of dry toluene under an argon atmosphere. The reaction flask was evacuated and refilled with argon three times. 9.88 g (0.104 mol) of chlorodimethylsilane and 3.0 ml Pt(dvs) (2mM solution in toluene) were added via a syringe. The reaction mixture was stirred for 12 hours at room temperature, then filtered over silica gel to remove the catalyst and the solvent was evaporated under vacuum and a colourless oil was obtained.

Yield: 5.7 g (93%)

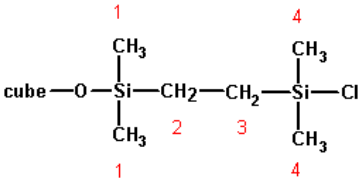

^{1}H NMR (δ, $CDCl_3$): 0.79-0.71 [bm, 16H, 3], 0.65-0.56 [bm, 16H, 2], 0.41 [s, 48H, 4], 0.17 [s, 48H, 1].

^{13}C NMR (δ, $CDCl_3$): 10.44 [3], 8.92 [2], 0.99 [4], -0.93 [1].

FT-IR (cm^{-1}): υ CH_3: 2961; υ CH_2: 2903; υ Si-CH_3: 1409, 1255, 825, 790; υ Si-C: 1171; υ Si-O: 1061; υ Si-Cl: 724, 636.

5.1.13. Preparation of octakis[(2-ethinyldimethylsilylethyl)dimethylsiloxy]octasil sesquioxane ($Q_8M_8^{alkyne}$)(9):

In a 50 ml round bottom flask equipped with an argon inlet, a reflux condenser and a magnetic stirrer 1.0 g (0.54 mmol) of $Q_8M_8^{Cl}$ (8) was dissolved in 10 ml of dry THF under an argon atmosphere. 17.1 ml of ethinyl magnesiumbromide (0.5 M solution in THF, 8.56 mmol) was added via a syringe. The reaction mixture was stirred for 3 hours at 40 °C, then diluted with diethyl ether and washed with saturated NaCl. The aqueous layer was washed two times with diethyl ether and the combined organic layers were dried over $MgSO_4$. The solvent was evaporated from the filtered solution and a yellow oil was obtained.

Yield: 0.74 g (78 %)

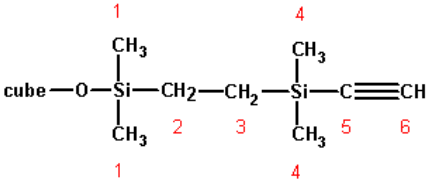

^{1}H NMR (δ, $CDCl_3$): 2.36 [s, 8H, 6], 0.57 [s, 32H, 2+3], 0.17 [s, 48H, 4], 0.14 [s, 48H, 1].
^{13}C NMR (δ, $CDCl_3$): 93.5 [6], 89.2 [5], 9.46 [3], 7.21 [2], -0.91 [4], -2.46 [1].
^{29}Si NMR (δ, $CDCl_3$): 13.15 [Si 1], -13.09 [Si 4], -108.8 [Si-O-Si, cube].

FT-IR (cm^{-1}): υ CH_3: 2961; υ CH_2: 2908; υ alkyne: 2035, 671; υ Si-CH_3: 1409, 1254, 823, 786; υ Si-C: 1169; υ Si-O (cage): 1064.

5.2. Preparation of modified POSS

5.2.1. Preparation of Ethinyltriethoxysilane:

This compound was obtained according to the following procedure by *Shea et al.*[123]. In a 100 ml round bottom flask equipped with an argon inlet and a magnetic stirrer 2.0 g (9.9 mmol) of chlorotriethoxysilane was dissolved in 20 ml of dry THF under an argon atmosphere. Ethinyl magnesiumbromide (19.9 ml of 0.5 M solution in THF, 9.9 mmol) was added via a syringe and the reaction mixture was stirred at room temperature for 24 hours. The solvent was evaporated under reduced pressure. The remaining brown oil was dissolved in diethyl ether, washed with water and saturated NaCl and dried over $MgSO_4$. The solvent was evaporated from the filtered solution. The pure product was obtained as a colourless liquid after vacuum-distillation.

Yield: 0.5 g (53%)

^{1}H NMR (δ, $CDCl_3$): 3.87 [q, J=7.03Hz, 6H, O-$\underline{CH_2}$-CH_3], 2.37 [s, 1H, C-$\underline{CH}$], 1.26 [t, 9H, J=6.97Hz, O-CH_2-$\underline{CH_3}$]. ^{13}C NMR (δ, $CDCl_3$): 92.8 [C≡$\underline{CH}$], 91.7 [$\underline{C}$≡CH], 58.9 [O-$\underline{CH_2}$-CH_3], 17.7 [O-CH_2-$\underline{CH_3}$].

FT-IR (cm^{-1}): υ CH_3: 2978, 1391; υ O-CH_2: 2930, 2895, 1447, 963; υ alkyne: 2051, 1296, 693; υ Si-C: 1155; υ Si-O: 1059; υ CH_2-CH_3: 742

5.2.2. Condensation of Ethinyltriethoxysilane with TBAF:

This reaction was performed according to the following procedure by *Bassindale et al.*[53]. In a 50 ml round bottom flask equipped with an argon inlet and a magnetic stirrer 0.5 g (2.7 mmol) of ethinyltriethoxysilane was dissolved in dry toluene under an argon atmosphere. Tetrabutylammoniumfluoride (0.9 ml of a 1 M solution in THF, 0.9 mmol) was added via a syringe and the reaction mixture was stirred 24 hours at room temperature. The white precipitate was removed from the solution and characterized by FT-IR. The solvent was evaporated from the solution under reduced pressure.

Characterization data of the soluble compound: ^{1}H NMR (δ, $CDCl_3$): 3.33 [t, J=8.23Hz, 2H, N-CH_2], 1.64 [p, J=7.03Hz, 2H, N-CH_2-CH_2], 1.45 [s, 2H, J=7.25Hz, N-CH_2-CH_2-CH_2], 0.98 [t, J=7.22Hz, 3H, CH_2-CH_3].
^{13}C NMR (δ, $CDCl_3$): 60.3 [N-CH_2], 25.5 [N-CH_2-CH_2], 21.3 [N-CH_2-CH_2-CH_2], 14.9 [CH_2-CH_3].
FT-IR (cm^{-1}): υ CH_3: 2959, 1378, 884; υ O-CH_2: 2873, 1476, 884; υ C-N^+: 1661, 1153, 1105; υ N-CH_2: 1378

Characterization data of the insoluble compound: FT-IR (cm^{-1}): υ CH_3: 2958; υ Si-O: broad 900-1250.

5.2.3. Preparation of octakis[2-(ethinyldimethylsilyl)ethyl]octasiloxane ($POSS^{alkyne}$) (10):

In a 50 ml round bottom flask equipped with an argon inlet, a reflux condenser and a magnetic stirrer 0.2 g (0.1 mmol) of $POSS^{Cl}$ was dissolved in 10 ml of dry THF under an argon atmosphere. Ethinyl magnesiumbromide (4.61 ml 0.5 M solution in THF, 2.3 mmol) was added via a syringe. The reaction mixture was stirred for 3 hours at 40°C, then diluted with diethyl ether and washed with saturated NaCl. The aqueous layer was washed two times with diethyl ether and the combined organic layers were dried over $MgSO_4$. The solvent was evaporated from the filtered solution and a white solid was obtained.

Yield: 0.14 g (74%)

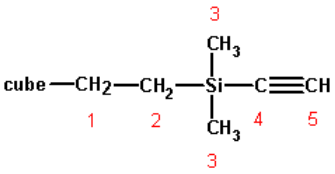

^{1}H NMR (δ, $CDCl_3$): 2.38 [s, 8H, 5], 0.66 [s, 16H, 1+2], 0.18 [s, 48H, 3].

^{13}C NMR (δ, $CDCl_3$): 93.6 [5], 89.0 [4], 7.5 [2], 4.2 [1], 1.0 [3].

^{29}Si NMR (δ, $CDCl_3$): -13.2 [Si 3], -66.8 [Si-O-Si, cage].

FT-IR (cm^{-1}): υ CH_3: 2966; υ CH_2: 2897; υ alkyne: 2040, 671; υ Si-CH_3: 1410, 1263, 847, 810; υ Si-C: 1110; υ Si-O: 1056.

5.3. Preparation of alkyne and azide modified Polymers

5.3.1. Preparation of alkyne end-modified Polydimethylsiloxane (11):

In a 50 ml round bottom flask equipped with an argon inlet and a magnetic stirrer 0.5 g (0.17 mmol) of chlorine end-modified polydimethylsiloxane ($PDMS^{Cl}$) was dissolved in 10 ml of dry THF under an argon atmosphere. 1.33 ml of ethinyl magnesiumbromide (0.5 M solution in THF, 0.67 mmol) was added via a syringe. The reaction mixture was stirred for 3 hours at room temperature, then diluted with diethyl ether and washed with saturated NaCl. The aqueous layer was washed two times with diethyl ether and the combined organic layers were dried over $MgSO_4$. The solvent was evaporated from the filtered solution and the product was obtained as a brown oil.

Yield: 0.37 g (74%)

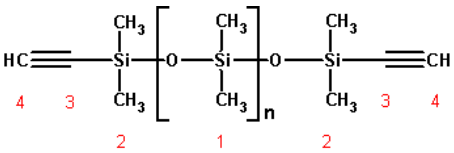

^{1}H NMR (δ, $CDCl_3$): 2.38 [s, 1H, 4], 0.23 [s, 24H, 2], 0.07 [s, 158H, 1].

^{13}C NMR (δ, $CDCl_3$): 91.9 [4], 89.3 [3], 2.01 [2], 1.04 [1].

^{29}Si NMR (δ, $CDCl_3$): -23.8 [1], -21.5 [2].

FT-IR (cm^{-1}): υ CH_3: 2964; υ alkyne: 2040, 688; υ Si-CH_3: 1408, 1260, 852, 790; υ Si-C: 1097; υ Si-O: 1019.

5.3.2. General procedure for the preparation of azide end-modified Poly(methyl methacrylate) (12):

This compound was obtained according to a procedure by *Altintas et al.*[99]. MMA, PMDETA, CuBr and EiBr in 10 ml of dry toluene were added in that order to a Schlenk tube under an argon atmosphere. The tube was degassed by three freeze-pump-thaw cycles, left in vacuum and placed in a thermostated oil bath at 80 °C for 5 min. Then the polymerization mixture was diluted with tetrahydrofurane and passed through a basic alumina column to remove the catalyst. Solvent was evaporated until only 20 ml of polymer solution was left and the polymer was precipitated in hexane. The polymer was dried at room temperature under reduced pressure for 24 hours.

[MMA]/[Initiator]		**100**	**50**	**30**
MMA		14.1 g (0.14 mol)	12.2 g (0.12 mol)	14.1 g (0.14 mol)
PMDETA		0.24 g (1.4 mmol)	0.42 g (2.4 mmol)	0.81 g (4.7 mmol)
CuBr		0.20 g (1.4 mmol)	0.35 g (2.4 mmol)	0.67 g (4.7 mmol)
EiBr		0.28 g (1.4 mmol)	0.48 g (2.4 mmol)	0.92 g (4.7 mmol)
SEC	**M_N**	4243	2325	1670
	PDI	1.49	1.44	1.39

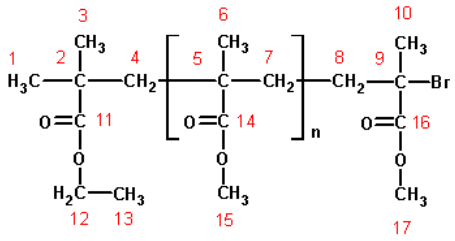

^{1}H NMR (δ, $CDCl_3$): 4.05 [q, J=7.00Hz, 12], 3.57 [s, 15], 1.7-2.0 [s, 7], 0.8-1.4 [s, 6].
^{13}C NMR (δ, $CDCl_3$): 177.5 [11, 14, 16], 60.2 [12], 57.0 [9], 54.1 [7], 51.5 [15+17], 45.5 [4+8], 44.2 [5], 41.1 [2], 29.7 + 21.9 [1+3], 27.5 [10], 18.4 + 16.1 [6], 13.8 [13].

FT-IR (cm^{-1}): υ C=O: 3438, 1733; υ CH_3: 2997, 2952; υ O-CH_3: 1447; υ C-CH_3: 1387; υ C-$(CR)_4$: 1251, 808; υ ester: 1151, 987.

The obtained PMMA was dissolved in 20 ml of dry DMF under an argon atmosphere. Sodium azide was added and stirred for 24 hours at room temperature. The reaction mixture was diluted with dichloromethane and washed three times with distilled water. The organic layer was dried over $MgSO_4$ and the solvent was evaporated from the filtered solution.

M_N	**4243**	**2325**	**1670**
PMMA	1.5 g (0.33 mmol)	1.5 g (0.65 mmol)	1.5 g (0.89 mmol)
NaN_3	0.43 g (6.67 mmol)	0.85 g (13.0 mmol)	1.17 g (17.9 mmol)

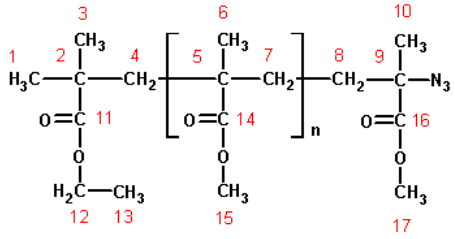

^{1}H NMR (δ, $CDCl_3$): 4.05 [q, J=7.00Hz, 12], 3.57 [s, 15], 1.7-2.0 [s, 7], 0.8-1.4 [s, 6].
^{13}C NMR (δ, $CDCl_3$): 177.6 [11, 14, 16], 64.0 [9], 60.3 [12], 54.2 [7], 51.7 [15+17], 44.3 [5], 41.2 [2], 29.9 + 21.9 [1+3], 25.2 [10], 18.5 + 16.2 [6], 13.9 [13].

FT-IR (cm^{-1}): υ C=O: 3441, 1732, 1680; υ CH_3: 2998, 2953, 1391; υ N_3: 2120, 1270, 1189; υ CH_2: 1480; υ O-CH_3: 1447; υ C-$(CR)_4$: 1244, 810; υ ester: 1149, 988.

5.4. Click Reactions

5.4.1. Click reaction between $Q_8M_8^{alkyne}$ and 1-azidoadamantane (13):

In a 50 ml round bottom flask equipped with 0.22 g (0.12 mmol) of $Q_8M_8^{alkyne}$ and 0.35 g (1.96 mmol) of 1-azidoadamantane were dissolved in 10 ml of dry DMF under an argon atmosphere. 0.15 ml of distilled water were added, followed by addition of 0.04 g (0.08 mmol) of tris(benzyltriazolylmethyl)amine and 0.02 g (0.06 mmol) of tetrakis(acetonitrile)copper(I)hexafluorophosphate. The reaction mixture was stirred at room temperature for 48 hours. The solvent was evaporated and the product was purified by column chromatography ($CHCl_3$:MeOH = 20:1).

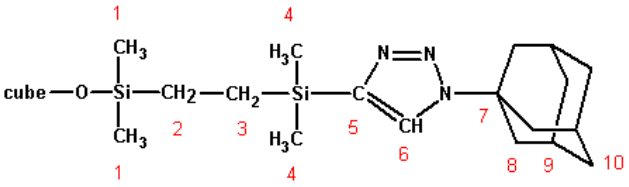

^{1}H NMR (δ, $CDCl_3$): 7.5 [s, 1H, 6], 2.25 [s, 10H, 8], 1.79 [s, 3H, 9], 0.46 [s, 4H, 2+3], 0.10 [s, 12H, 1+4].

^{13}C NMR (δ, $CDCl_3$): 144 [5], 133 [6], 125 [6], 119 [6], 43 [8], 42 [9], 30 [10], 9 [2], 7[3], 0 [1], -4 [4].

FT-IR (cm^{-1}): υ triazole: 3121, 2670, 2481, 1356, 1309; υ azide (residual): 2135; υ alkyne (residual): 2087; υ Si-CH_3: 1449, 1253, 823, 786; υ Si-C: 1137; υ Si-O: 1083.

6. References

(1) Sharp, K. G. *Adv. Mater.* **1998**, *10*, 1243-1248.

(2) Sanchez, C.; Julian, B.; Belleville, P.; Popall, M. *J. Mater. Chem.* **2005**, *15*, 3559-3592.

(3) Mammeri, F.; Le Bourhis, E.; Rozes, L.; Sanchez, C. *J. Mater. Chem.* **2005**, *15*, 3787-3811.

(4) Su, H.-W.; Chen, W.-C.; Lee, W.-C.; King, J.-S. *Macromol. Mater. Eng.* **2007**, *292*, 666-673.

(5) Naga, N.; Oda, E.; Toyota, A.; Horie, K.; Furukawa, H. *Macromol. Chem. Phys.* **2006**, *207*, 627-635.

(6) Lligadas, G.; Callau, L.; Ronda, J. C.; Galia, M.; Cadiz, V. *J. Polym. Sci., Part A: Polym. Chem.* **2005**, *43*, 6295-6307.

(7) Wada, K.; Watanabe, N.; Yamada, K.; Kondo, T.; Mitsudo, T.-a. *Chem. Commun.* **2005**, 95-97.

(8) Zheng, L.; Farris, R. J.; Coughlin, E. B. *Macromolecules* **2001**, *34*, 8034-8039.

(9) Toepfer, O.; Neumann, D.; Choudhury, N. R.; Whittaker, A.; Matisons, J. *Chem. Mater.* **2005**, *17*, 1027-1035.

(10) Holzinger, D.; Kickelbick, G. *J. Polym. Sci., Part A: Polym. Chem.* **2002**, *40*, 3858-3872.

(11) Kickelbick, G.; Schubert, U. *Monatsh. Chem.* **2001**, *132*, 13-30.

(12) Kickelbick, G. *Angew. Chem. Int. Ed.* **2004**, *43*, 3102-3104.

(13) Smaihi, M.; Hovnanian, N. *Recent Research Developments in Applied Polymer Science* **2002**, *1*, 387-427.

(14) Coronado, E.; Galan-Mascaros, J. R. *J. Mater. Chem.* **2005**, *15*, 66-74.

(15) Rabu, P.; Drillon, M. *Functional Hybrid Materials* **2004**, 270-316.

(16) Bourbigot, S.; Duquesne, S.; Jama, C. *Macromol. Symp.* **2006**, *233*, 180-190.

(17) Weiner, S.; Traub, W.; Wagner, H. D. *J Struct Biol FIELD Full Journal Title:Journal of structural biology* **1999**, *126*, 241-55.

(18) Spoto, G.; Torrisi, A.; Contino, A. *Chem. Soc. Rev.* **2000**, *29*, 429-439.

(19) Innocenzi, P.; Lebeau, B. *J. Mater. Chem.* **2005**, *15*, 3821-3831.

(20) Williams, K. A.; Boydston, A. J.; Bielawski, C. W. *Chem. Soc. Rev.* **2007**, *36*, 729-744.

(21) Gomez-Romero, P.; Cuentas-Gallegos, K.; Lira-Cantu, M.; Casan-Pastor, N. *J. Mater. Sci.* **2005**, *40*, 1423-1428.

(22) Licoccia, S.; Traversa, E. *J. Power Sources* **2006**, *159*, 12-20.

(23) Forster, P. M.; Cheetham, A. K. *Top. Catal.* **2003**, *24*, 79-86.

(24) Tsuru, K.; Hayakawa, S.; Osaka, A. *Hybrid Materials* **2007**, 301-335.

(25) Schottner, G.; Rose, K.; Posset, U. *J. Sol-Gel Sci. Technol.* **2003**, *27*, 71-79.

(26) Arici, E.; Sariciftci, N. S.; Meissner, D. *Encyclopedia of Nanoscience and Nanotechnology* **2004**, *3*, 929-944.

(27) Baldi, F.; Bignotti, F.; Fina, A.; Tabuani, D.; Ricco, T. *J. Appl. Polym. Sci.* **2007**, *105*, 935-943.

(28) Kickelbick, G. *Prog. Polym. Sci.* **2002**, *28*, 83-114.

(29) Li, G.; Wang, L.; Ni, H.; Pittman, C. U., Jr. *J. Inorg. Organomet. Polym.* **2002**, *11*, 123-154.

(30) Tamaki, R.; Choi, J.; Laine, R. M. *Chem. Mater.* **2003**, *15*, 793-797.
(31) Sanchez, C.; de Soler-Illia, G. J.; Ribot, F.; Lalot, T.; Mayer, C. R.; Cabuil, V. *Chem. Mater.* **2001**, *13*, 3061-3083.
(32) Roduner, E. *Chem. Soc. Rev.* **2006**, *35*, 583-592.
(33) Choi, J.; Harcup, J.; Yee, A. F.; Zhu, Q.; Laine, R. M. *JACS* **2001**, *123*, 11420-11430.
(34) Binder, W. H.; Petraru, L.; Sachenshofer, R.; Zirbs, R. *Monatsh. Chem.* **2006**, *137*, 835-841.
(35) Kannan, R. Y.; Salacinski, H. J.; Butler, P. E.; Seifalian, A. M. *Acc. Chem. Res.* **2005**, *38*, 879-884.
(36) Kickelbick, G. *Chem. unserer Zeit* **2005**, *39*, 46-53.
(37) Laine, R. M.; Zhang, C.; Sellinger, A.; Viculis, L. *Appl. Organomet. Chem.* **1998**, *12*, 715-723.
(38) Schwab, J. J.; Lichtenhan, J. D. *Appl. Organomet. Chem.* **1998**, *12*, 707-713.
(39) Sellinger, A.; Laine, R. M. *Macromolecules* **1996**, *29*, 2327-30.
(40) Sheng, Y.-J.; Lin, W.-J.; Chen, W.-C. *J. Chem. Phys.* **2004**, *121*, 9693-9701.
(41) Angot, S.; Taton, D.; Gnanou, Y. *Macromolecules* **2000**, *33*, 5418-5426.
(42) Hoebbel, D.; Wieker, W. *Z. Anorg. Allg. Chem.* **1971**, *384*, 43-52.
(43) Hasegawa, I.; Kuroda, K.; Kato, C. *Bull. Chem. Soc. Jpn.* **1986**, *59*, 2279-83.
(44) Hoebbel, D.; Weber, C.; Schmidt, H.; Krueger, R.-P. *J. Sol-Gel Sci. Technol.* **2002**, *24*, 121-129.
(45) Hasegawa, I.; Ishida, M.; Motojima, S. *Synth. React. Inorg. Met.-Org. Chem.* **1994**, *24*, 1099-110.
(46) Harrison, P. G.; Hall, C. *Main Group Met. Chem.* **1997**, *20*, 515-529.
(47) Laine, R. M. *J. Mater. Chem.* **2005**, *15*, 3725-3744.
(48) Hasegawa, I.; Niwa, T.; Takayama, T. *Inorg. Chem. Commun.* **2005**, *8*, 159-161.
(49) Ladenburg *Chem. Ber.* **1873**, *6*, 130.
(50) Scott, D. W. *JACS* **1946**, *68*, 356-8.
(51) Barry, A. J.; Daudt, W. H.; Domicone, J. J.; Gilkey, J. W. *JACS* **1955**, *77*, 4248-52.
(52) Brown, J. F., Jr.; Vogt, L. H., Jr.; Prescott, P. I. *JACS* **1964**, *86*, 1120-5.
(53) Bassindale, A. R.; Parker, D. J.; Pourny, M.; Taylor, P. G.; Horton, P. N.; Hursthouse, M. B. *Organometallics* **2004**, *23*, 4400-4405.
(54) Brown, J. F., Jr.; Vogt, L. H., Jr. *JACS* **1965**, *87*, 4313-17.
(55) Speier, J. L.; Webster, J. A.; Barnes, G. H. *JACS* **1957**, *79*, 974-9.
(56) Chalk, A. J.; Harrod, J. F. *JACS* **1965**, *87*, 16-21.
(57) Roy, A. K.; Taylor, R. B. *JACS* **2002**, *124*, 9510-9524.
(58) Pielichowski, K.; Njuguna, J.; Janowski, B.; Pielichowski, J. *Adv. Polym. Sci.* **2006**, *201*, 225-296.
(59) Lee, A.; Xiao, J.; Feher, F. J. *Macromolecules* **2005**, *38*, 438-444.
(60) Zheng, L.; Kasi, R. M.; Farris, R. J.; Coughlin, E. B. *J. Polym. Sci., Part A: Polym. Chem.* **2002**, *40*, 885-891.
(61) Kim, K.-M.; Ouchi, Y.; Chujo, Y. *Polym. Bull.* **2003**, *49*, 341-348.
(62) Harris, H.; Lamy, Y.; Lutz, P. J. *Polym. Prepr. (Am. Chem. Soc., Div. Polym. Chem.)* **2006**, *47*, 551-552.
(63) Neumann, D.; Fisher, M.; Tran, L.; Matisons, J. G. *JACS* **2002**, *124*, 13998-13999.

(64) Zhang, C.; Bunning, T. J.; Laine, R. M. *Chem. Mater.* **2001**, *13*, 3653-3662.
(65) Nyman, M. D.; Desu, S. B.; Peng, C. H. *Chem. Mater.* **1993**, *5*, 1636-40.
(66) Gonsalves, K. E.; Merhari, L.; Wu, H.; Hu, Y. *Adv. Mater.* **2001**, *13*, 703-714.
(67) Hawker, C. J.; Bosman, A. W.; Harth, E. *Chem. Rev.* **2001**, *101*, 3661-3688.
(68) Wang, J.-S.; Matyjaszewski, K. *JACS* **1995**, *117*, 5614-15.
(69) Tomalia, D. A.; Frechet, J. M. J. *J. Polym. Sci., Part A: Polym. Chem.* **2002**, *40*, 2719-2728.
(70) Zhang, H.; Jiang, X.; van der Linde, R. *Polymer* **2004**, *45*, 1455-1466.
(71) Bon, S. A. F.; Steward, A. G.; Haddleton, D. M. *J. Polym. Sci., Part A: Polym. Chem.* **2000**, *38*, 2678-2686.
(72) Coessens, V.; Matyjaszewski, K. *Macromol. Rapid Commun.* **1999**, *20*, 66-70.
(73) Malz, H.; Komber, H.; Voigt, D.; Hopfe, I.; Pionteck, J. *Macromol. Chem. Phys.* **1999**, *200*, 642-651.
(74) Coessens, V.; Matyjaszewski, K. *J. Macromol. Sci., Pure Appl. Chem.* **1999**, *A36*, 667-679.
(75) Matyjaszewski, K.; Nakagawa, Y.; Gaynor, S. G. *Macromol. Rapid Commun.* **1997**, *18*, 1057-1066.
(76) Kolb, H. C.; Finn, M. G.; Sharpless, K. B. *Angew. Chem. Int. Ed.* **2001**, *40*, 2004-2021.
(77) Kolb, H. C.; Sharpless, K. B. *Drug Discovery Today* **2003**, *8*, 1128-1137.
(78) Opsteen, J. A.; van Hest, J. C. M. *Chem. Commun.* **2005**, 57-59.
(79) Binder, W. H.; Sachsenhofer, R. *Macromol. Rapid Commun.* **2007**, *28*, 15-54.
(80) Nandivada, H.; Jiang, X.; Lahann, J. *Adv. Mater.* **2007**, *19*, 2197-2208.
(81) Huisgen, R. *Angew. Chem.* **1963**, *75*, 604-37.
(82) Huisgen, R. *Angew. Chem.* **1963**, *75*, 742-54.
(83) Huisgen, R. *Angew. Chem. Int. Ed.* **1968**, *7*, 321-8.
(84) Firestone, R. A. *J. Org. Chem.* **1968**, *33*, 2285-90.
(85) Firestone, R. A. *J. Org. Chem.* **1972**, *37*, 2181-91.
(86) McDouall, J. J. W.; Robb, M. A.; Niazi, U.; Bernardi, F.; Schlegel, H. B. *JACS* **1987**, *109*, 4642-8.
(87) Rostovtsev, V. V.; Green, L. G.; Fokin, V. V.; Sharpless, K. B. *Angew. Chem. Int. Ed.* **2002**, *41*, 2596-2599.
(88) Rodionov, V. O.; Fokin, V. V.; Finn, M. G. *Angew. Chem. Int. Ed.* **2005**, *44*, 2210-2215.
(89) Rodionov, V. O.; Presolski, S. I.; Diaz, D. D.; Fokin, V. V.; Finn, M. G. *JACS* **2007**, *129*, 12705-12712.
(90) Himo, F.; Lovell, T.; Hilgraf, R.; Rostovtsev, V. V.; Noodleman, L.; Sharpless, K. B.; Fokin, V. V. *JACS* **2005**, *127*, 210-216.
(91) Himo, F.; Demko, Z. P.; Noodleman, L.; Sharpless, K. B. *JACS* **2002**, *124*, 12210-12216.
(92) Ahlquist, M.; Fokin, V. V. *Organometallics* **2007**, *26*, 4389-4391.
(93) Chan, T. R.; Hilgraf, R.; Sharpless, K. B.; Fokin, V. V. *Org. Lett.* **2004**, *6*, 2853-2855.
(94) Chassaing, S.; Kumarraja, M.; Sido, A. S. S.; Pale, P.; Sommer, J. *Org. Lett.* **2007**, *9*, 883-886.

(95) Aucagne, V.; Berna, J.; Crowley, J. D.; Goldup, S. M.; Haenni, K. D.; Leigh, D. A.; Lusby, P. J.; Ronaldson, V. E.; Slawin, A. M. Z.; Viterisi, A.; Walker, D. B. *JACS* **2007**, *129*, 11950-11963.

(96) Rodionov, V. O.; Presolski, S. I.; Gardinier, S.; Lim, Y.-H.; Finn, M. G. *JACS* **2007**, *129*, 12696-12704.

(97) Tornoe, C. W.; Christensen, C.; Meldal, M. *J. Org. Chem.* **2002**, *67*, 3057-3064.

(98) Moses John, E.; Moorhouse Adam, D. *Chem. Soc. Rev.* **2007**, *36*, 1249-62.

(99) Altintas, O.; Yankul, B.; Hizal, G.; Tunca, U. *J. Polym. Sci., Part A: Polym. Chem.* **2006**, *44*, 6458-6465.

(100) Fournier, D.; Hoogenboom, R.; Schubert, U. S. *Chem. Soc. Rev.* **2007**, *36*, 1369-1380.

(101) Golas, P. L.; Tsarevsky, N. V.; Sumerlin, B. S.; Matyjaszewski, K. *Macromolecules* **2006**, *39*, 6451-6457.

(102) Lutz, J.-F. *Angew. Chem. Int. Ed.* **2007**, *46*, 1018-1025.

(103) Sumerlin, B. S.; Tsarevsky, N. V.; Louche, G.; Lee, R. Y.; Matyjaszewski, K. *Macromolecules* **2005**, *38*, 7540-7545.

(104) Tsarevsky, N. V.; Sumerlin, B. S.; Matyjaszewski, K. *Macromolecules* **2005**, *38*, 3558-3561.

(105) Vogt, A. P.; Sumerlin, B. S. *Macromolecules* **2006**, *39*, 5286-5292.

(106) Brase, S.; Gil, C.; Knepper, K.; Zimmermann, V. *Angew. Chem. Int. Ed.* **2005**, *44*, 5188-5240.

(107) Curtius, T. *Journal fuer Praktische Chemie (Leipzig)* **1894**, *50*, 275-94.

(108) Hantzsch, A. *Ber.* **1933**, *66B*, 1349-54.

(109) Petraru, L.; Binder, W. H. *Polym. Prepr. (Am. Chem. Soc., Div. Polym. Chem.)* **2005**, *46*, 841-842.

(110) Hoebbel, D.; Pitsch, I.; Grimmer, A. R.; Jancke, H.; Hiller, W.; Harris, R. K. *Zeitschrift fuer Chemie* **1989**, *29*, 260-1.

(111) Provatas, A.; Luft, M.; Mu, J. C.; White, A. H.; Matisons, J. G. *J. Organomet. Chem.* **1998**, *565*, 159-164.

(112) Jankowiak, M.; Maciejewski, H.; Gulinski, J. *J. Organomet. Chem.* **2005**, *690*, 4478-4487.

(113) Zhang, C.; Laine, R. M. *JACS* **2000**, *122*, 6979-6988.

(114) Nummert, V.; Piirsalu, M.; Maemets, V.; Koppel, I. *J. Phys. Org. Chem.* **2005**, *18*, 1138-1144.

(115) Hasegawa, I.; Nakane, Y.; Takayama, T. *Appl. Organomet. Chem.* **1999**, *13*, 273-277.

(116) Jutzi, P.; Batz, C.; Mutluay, A. *Z. Naturforsch., B: Chem. Sci.* **1994**, *49*, 1689-92.

(117) Frisch, K. C.; Young, R. B. *JACS* **1952**, *74*, 4853-6.

(118) Hiroya, K.; Jouka, R.; Kameda, M.; Yasuhara, A.; Sakamoto, T. *Tetrahedron* **2001**, *57*, 9697-9710.

(119) Bassindale, A. R.; Chen, H.; Liu, Z.; MacKinnon, I. A.; Parker, D. J.; Taylor, P. G.; Yang, Y.; Light, M. E.; Horton, P. N.; Hursthouse, M. B. *J. Organomet. Chem.* **2004**, *689*, 3287-3300.

(120) Ettenhuber, E.; Ruehlmann, K. *Chem. Ber.* **1968**, *101*, 743-50.

(121) Coessens, V.; Nakagawa, Y.; Matyjaszewski, K. *Polym. Bull.* **1998**, *40*, 135-142.

(122) Hasegawa, I.; Motojima, S. *J. Organomet. Chem.* **1992**, *441*, 373-80.

(123) Shea, K. J.; Loy, D. A.; Webster, O. *JACS* **1992**, *114*, 6700-10.